AD-A114 793 BATTELLE COLUMBUS LABS OH F/G 11/6
SHEAR BANDS IN FORGED PRODUCTS.(U)
MAR 82 S L SEMIATIN, G D LAHOTI, S I OH AFOSR-79-0048
UNCLASSIFIED AFOSR-TR-82-0392 NL

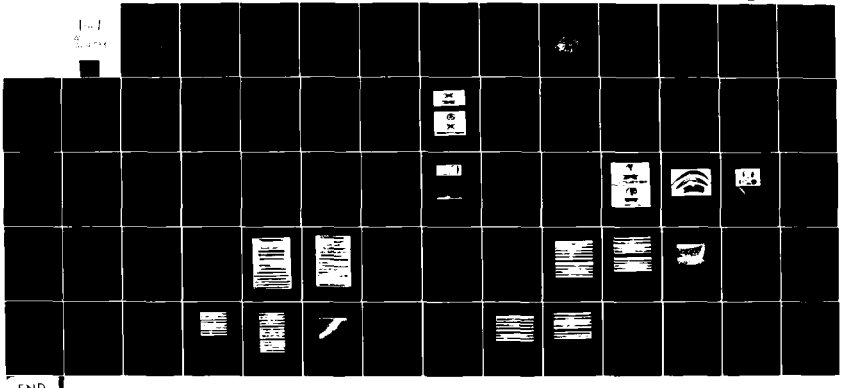

END
DATE FILMED
6 82
DTIC

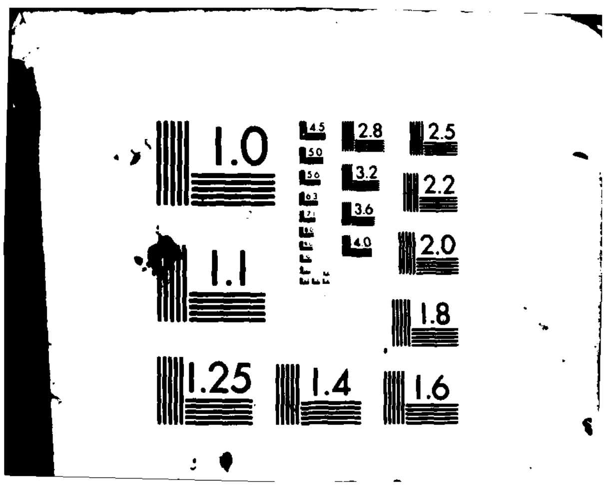
1.0
2.8
2.5
3.2
2.2
3.6
4.0
2.0
1.1
1.8
1.25
1.4
1.6

UNCLASSIFIED
SECURITY CLASSIFICATION OF THIS PAGE (When Data Entered)

G 8287 (11)

REPORT DOCUMENTATION PAGE		READ INSTRUCTIONS BEFORE COMPLETING FORM
1. REPORT NUMBER AFOSR-TR- 82-0392	2. GOVT ACCESSION NO. AD-A114793	3. RECIPIENT'S CATALOG NUMBER
4. TITLE (and Subtitle) SHEAR BANDS IN FORGED PRODUCTS		5. TYPE OF REPORT & PERIOD COVERED FINAL TECHNICAL (1979-1982)
		6. PERFORMING ORG. REPORT NUMBER
7. AUTHOR(s) S. L. SEMIATIN, G. D. LAHOTI, S. I. OH, A. L. HOFFMANNER, AND T. ALTAN		8. CONTRACT OR GRANT NUMBER(s) AFOSR-79-0048
9. PERFORMING ORGANIZATION NAME AND ADDRESS BATTELLE'S COLUMBUS LABORATORIES 505 KING AVENUE COLUMBUS, OHIO 43201		10. PROGRAM ELEMENT, PROJECT, TASK AREA & WORK UNIT NUMBERS 2306/A1 61102F
11. CONTROLLING OFFICE NAME AND ADDRESS AIR FORCE OFFICE OF SCIENTIFIC RESEARCH/NE DIRECTORATE OF ELECTRONIC AND SOLID STATE SCIENCES BOLLING AIR FORCE BASE, D.C. 20332		12. REPORT DATE MARCH, 1982
		13. NUMBER OF PAGES 65
14. MONITORING AGENCY NAME & ADDRESS(if different from Controlling Office)		15. SECURITY CLASS. (of this report) UNCLASSIFIED
		15a. DECLASSIFICATION/DOWNGRADING SCHEDULE N.A.

16. DISTRIBUTION STATEMENT (of this Report)

Approved for public release; distribution unlimited.

17. DISTRIBUTION STATEMENT (of the abstract entered in Block 20, if different from Report)

18. SUPPLEMENTARY NOTES

19. KEY WORDS (Continue on reverse side if necessary and identify by block number)

Titanium alloys, shear bands. localized deformation, instability, flow softening, hot torsion, lateral sidepressing, conventional forging, isothermal forging, hot forging, localization parameter, heat transfer, shear band fracture, tensile behavior, creep behavior, and fatigue behavior.

20. ABSTRACT (Continue on reverse side if necessary and identify by block number)

Shear bands, intense bands of localized deformation, are a primary source of defective forgings and their occurrence is a significant factor limiting the precision attainable by forging. During this program, the occurrence of shear bands in both isothermal, hot forging and conventional, non-isothermal hot forging has been determined for the alloy Ti-6Al-2Sn-4Zr-2Mo-0.1 Si (Ti-6242). Lateral sidepressing of Ti-6242 cylinders was used to determine the strain rate and temperature regimes in which shear bands may develop during isothermal, hot forging. From these observations, workability maps,

DD FORM 1 JAN 73 1473

UNCLASSIFIED
SECURITY CLASSIFICATION OF THIS PAGE (When Data Entered)

denoting process conditions which lead to shear bands were developed. A simple instability model based on these data and observations of shear localization in torsion tests was used in conjunction with measured material data to interpret the results. This model established the important influence of the flow localization parameter α (ratio of the work softening rate to the strain-rate sensitivity parameter) on the tendency to form shear bands. More in-depth analysis, making use of an advanced computer code, confirmed the applicability of the simple instability model and established the capability of describing the detailed process by which shear bands initiate as well as propagate. Uniaxial compression of cylinders, lateral sidepressing of cylinders, and forging of an airfoil shape were employed to document the occurrence of shear bands in non-isothermal (conventional), hot forging of Ti-6242. Run in mechanical and hydraulic presses, these forging operations established working speed as the most important process variable affecting the die chilling which controls the development of shear bands non-isothermally. Even though shear bands occurred at both mechanical as well as hydraulic press speeds, the deformation at the low hydraulic press speed was so severe as to lead to fracturing along the shear bands. Other process variables such as lubrication, dwell time, preheat temperature, and die temperature were also found to have some influence on heat transfer and die chilling and, hence, on the severity of flow localization. A simple analysis was used to rationalize these observations and, offer direction for more detailed process simulation of non-isothermal forging. Lastly, the effect of shear bands in forged products of Ti-6242 on service properties was determined. Characterization of tensile, fatigue, and creep properties on forgings containing shear bands was done at 510 C (950 F), the maximum operating temperature of Ti-6242 forgings in jet engines. From these tests, it was found that the effect of the shear bands was small. In the vast majority of the characterization tests, fracture initiation and fracture propagation sites lay in the homogeneously-deformed bulk of the forging and not at the shear bands. The effects of shear bands on properties that were observed, however, were ascribed to either the generally higher hardness of the shear bands as compared to the homogeneously-deformed bulk of the forgings (tensile properties) or enhanced diffusion along shear bands (creep properties).

AFOSR-TR- 82-0392

FINAL TECHNICAL REPORT

on

SHEAR BANDS IN FORGED PRODUCTS

(Grant No. AFOSR-79-0048)

to

DEPARTMENT OF THE AIR FORCE
AIR FORCE OFFICE OF SCIENTIFIC RESEARCH
BOLLING AIR FORCE BASE, D.C. 20332

March 15, 1982

by

S. L. Semiatin, G. D. Lahoti, S. I. Oh,
A. L. Hoffmanner, and T. Altan

BATTELLE
Columbus Laboratories
505 King Avenue
Columbus, Ohio 43201

FINAL TECHNICAL REPORT

on

SHEAR BANDS IN FORGED PRODUCTS
(Grant No. AFOSR-79-0048)

to

DEPARTMENT OF THE AIR FORCE
AIR FORCE OFFICE OF SCIENTIFIC RESEARCH
BOLLING AIR FORCE BASE, D.C. 20332

from

BATTELLE

Columbus Laboratories

by

S. L. Semiatin, G. D. Lahoti, S. I. Oh,
A. L. Hoffmanner, and T. Altan

March 15, 1982

ABSTRACT

Shear bands, intense bands of localized deformation, are a primary source of defective forgings and their occurrence is a significant factor limiting the precision attainable by forging. The occurrence and effects of shear bands are not well understood. There is no test for predicting their occurrence and, therefore, they are averted by the inefficient and costly use of oversize forgings and in-process die reworking. The overall objective of this program is to document the occurrence of shear bands in forged products produced under well defined conditions, develop analytical techniques for their prediction, and evaluate their effects on structural performance. The proposed approach is based on characterizing the deformation behavior of a titanium alloy, Ti-6242, of interest to the Air Force; employing the results of the characterization as input for a mathematical model of the deformation process to predict shear band formation; and evaluating the effects of shear bands on structural-test performance.

Lateral sidepressing of Ti-6Al-2Sn-4Zr-2Mo-0.1 Si (Ti-6242) cylinders was used to determine the strain rate and temperature regimes in which shear bands may develop during isothermal, hot forging. From these observations, workability maps, denoting process conditions which lead to shear bands were developed. A simple instability model based on these data and observations of shear localization in torsion tests was used in conjunction with measured material data to interpret the results. This model established the important influence of the flow localization parameter α (ratio of the work softening rate to the strain-rate sensitivity parameter) on the tendency to form shear bands. More in-depth analysis, making use of an advanced computer code, confirmed the applicability of the simple instability model and established the capability of describing the detailed process by which shear bands initiate as well as propagate.

Uniaxial compression of cylinders, lateral sidepressing of cylinders, and forging of an airfoil shape were employed to document the occurrence of shear bands in non-isothermal (conventional), hot forging of Ti-6242. Run in mechanical and hydraulic presses, these forging operations established working speed as the most important process variable affecting the die chilling which controls the development of shear bands non-isothermally. Even though shear bands occurred at both mechanical as well as hydraulic press speeds, the deformation at the low hydraulic press speed was so severe as to lead to fracturing along the shear bands. Other process variables such as lubrication, dwell time, preheat temperature, and die temperature were also found to have some influence on heat transfer and die chilling and, hence, on the severity of flow localization. A simple analysis was used to rationalize these observations and offer direction for more detailed process simulation of non-isothermal forging.

Lastly, the effect of shear bands in forged products of Ti-6242 on service properties was determined. Characterization of tensile, fatigue, and creep properties on forgings containing shear bands was done at 510 C (950 F), the maximum operating temperature of Ti-6242 forgings in jet engines. From these tests, it was found that the effect of the shear bands was small. In the vast majority of the characterization tests, fracture initiation and fracture propagation sites lay in the homogeneously deformed bulk of the forging and not at the shear bands. The small effects of shear

bands on properties that were observed, however, were ascribed to either the generally higher hardness of the shear bands as compared to the homogeneously-deformed bulk of the forgings (tensile properties) or enhanced diffusion along shear bands (creep properties).

SUMMARY OF RESULTS AND THEIR SIGNIFICANCE

This program was performed over a three-year period. The objectives of the first year's work were to characterize the program alloy, develop and validate deformation-heat transfer models, and establish instability criteria. These objectives were pursued under the following tasks:

Task 1. Materials Characterization

Task 2. Determination of Fracture Strains and Fracture Mode in Uniaxial Tension

Task 3. Deformation Heating and Heat Transfer Tests

Task 4. Simple Shear Deformation Trials (and Preliminary Shear Band Observations)

Task 5. Modeling of Heat Transfer and Deformation.

During the second year, the objective was to apply the deformation-heat transfer analysis and instability criteria to actual forging situations in order to predict the occurrence of shear bands. This work was conducted under the following tasks:

Task 1. Shear Bands in Isothermally-Forged Ti-6242

Task 2. Shear Bands in Non-Isothermally-Forged Ti-6242

Task 3. Shear Bands in a Complex Forging

Task 4. Analysis and Modeling.

The objective of the third year's program was to establish the effect of shear bands on service properties in forged products of Ti-6242. This objective was met by the following tasks:

Task 1. Generation of Shear Bands under Controlled Conditions

Task 2. Effect of Heat Treatment on Microstructures of Forged Samples With and Without Shear Bands

Task 3. Evaluation of Tensile Properties

Task 4. Evaluation of Creep Properties

Task 5. Evaluation of Fatigue Properties.

The results of the first two years of the program have been presented and discussed in detail in the first two yearly reports and several published papers. However, for completeness, they will be summarized under the major headings of (A) Materials Characterization, (B) Instability Criterion, (C) Shear Band Occurrence and Prediction in Isothermal Forging, and (D) Shear Band Occurrence and Prediction in Non-Isothermal Forging. Following this, the third year's results will be discussed under the general heading of The Effect of Shear Bands on Service Properties.

Materials Characterization

Materials Selection

After consultation with personnel at the Air Force Materials Laboratory (A. M. Adair, H. Gegel) and AFOSR, the titanium alloy Ti-6242 (Ti-6Al-2Sn-4Zr-2Mo-0.1 Si) was selected as the program alloy. This alloy is similar to Ti-64 (Ti-6Al-4V) but has a slightly higher operating temperature and is expected to be used increasingly in jet engines in coming years. Shear bands are common in $\alpha+\beta$ titanium alloys such as Ti-6242 and Ti-64. The Ti-6242 was supplied by Wyman-Cordon Company of North Grafton, Massachusetts, and met the AMS specification for forging bar stock. The material had been forged at 954 C (1750 F) and heat treated at 968 C (1775 F) yielding a microstructure of equiaxed α in a transformed β matrix, hereafter referred to as the $\alpha+\beta$ microstructure (Figure 1). Some of this material was heat treated at 1010 C (1850 F) for 30 minutes and air cooled to produce a transformed, acicular basketweave microstructure, hereafter referred to as the β microstructure (Figure 1). The β transus had been specified as 988 C (1810 F).

Compression Tests

Isothermal compression testing was used to characterize the stress-strain behavior of the program alloy. Compression testing was selected to provide stress-strain data at large strains for deformation analyses and

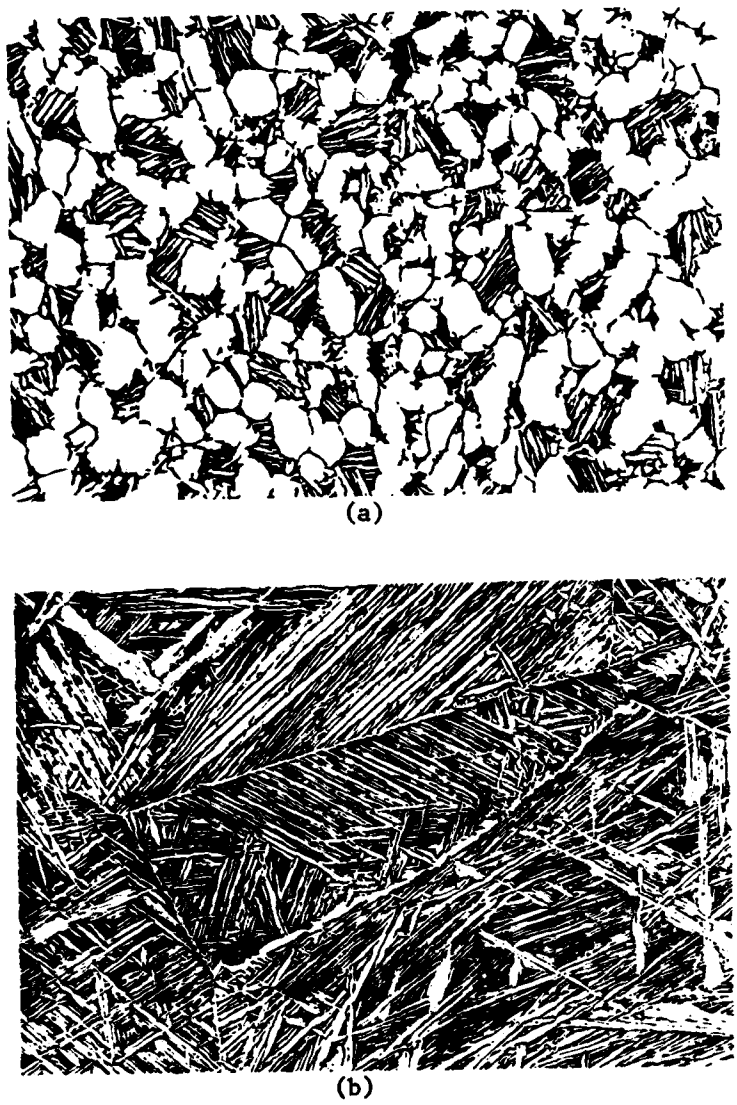

FIGURE 1. (a) α+β and (b) β Microstructures of Ti-6242 Program Alloy (500X)

because computer programs and verified analytical techniques exist at Battelle for accurate interpretation of the results. A test fixture with superalloy tooling was constructed with Battelle funds to run the hot, isothermal compression tests on an MTS machine (Figure 2). All testing was performed with test specimens precoated with glasses to provide lubrication and protection from the atmosphere. Specimens of both microstructures ($\alpha+\beta$ and β) were tested at constant true strain rates of 0.001, 0.1, 1.0, and 10.0 $sec.^{-1}$. The $\alpha+\beta$ microstructure was tested at 816, 871, 913, 954, and 1010 C (1500, 1600, 1675, 1750, and 1850 F). The β microstructure was characterized only at the first four of these temperatures since at 1010 C (1850 F), both microstructures revert to the single-phase bcc microstructure.

The compression data exhibited a marked difference in basic behavior between $\alpha+\beta$ and β microstructure material. The $\alpha+\beta$ load-stroke curves increased monotonically, whereas the β load-stroke curves were generally decreasing or constant with respect to stroke. Due to the non-increasing nature of the β load-stroke curves, compression specimens of this structure tended to deform non-uniformily, an observation similar to that made in mechanical-press-compression tests on this alloy for the disk program[1]. The difference in load-stroke curves for the two microstructures carried over to the stress-strain curves. The β stress-strain curves generally showed much larger degrees of flow softening[2] than the $\alpha+\beta$ stress-strain curves, an effect which was later found to be very important in the development of shear bands, particularly in isothermal forging.

Modeling of the deformation processes under investigation required knowledge of the flow stress as a function of strain, strain rate, and temperature. For this reason, the stress-strain data at a given strain rate were cross-plotted in terms of stress versus temperature at given levels of strain. Because of deformation heating, however, flow stress values at the higher strain levels for a test at a given nominal test temperature are actually representative of the deformation resistance at somewhat higher temperatures. The temperature rises were calculated assuming 95 percent of the deformation work (area under the stress-strain curve) was converted into heat. Sample stress-temperature data corrected for adiabatic heating are shown in Figure 3. It is seen that data for the $\alpha+\beta$ microstructure fall

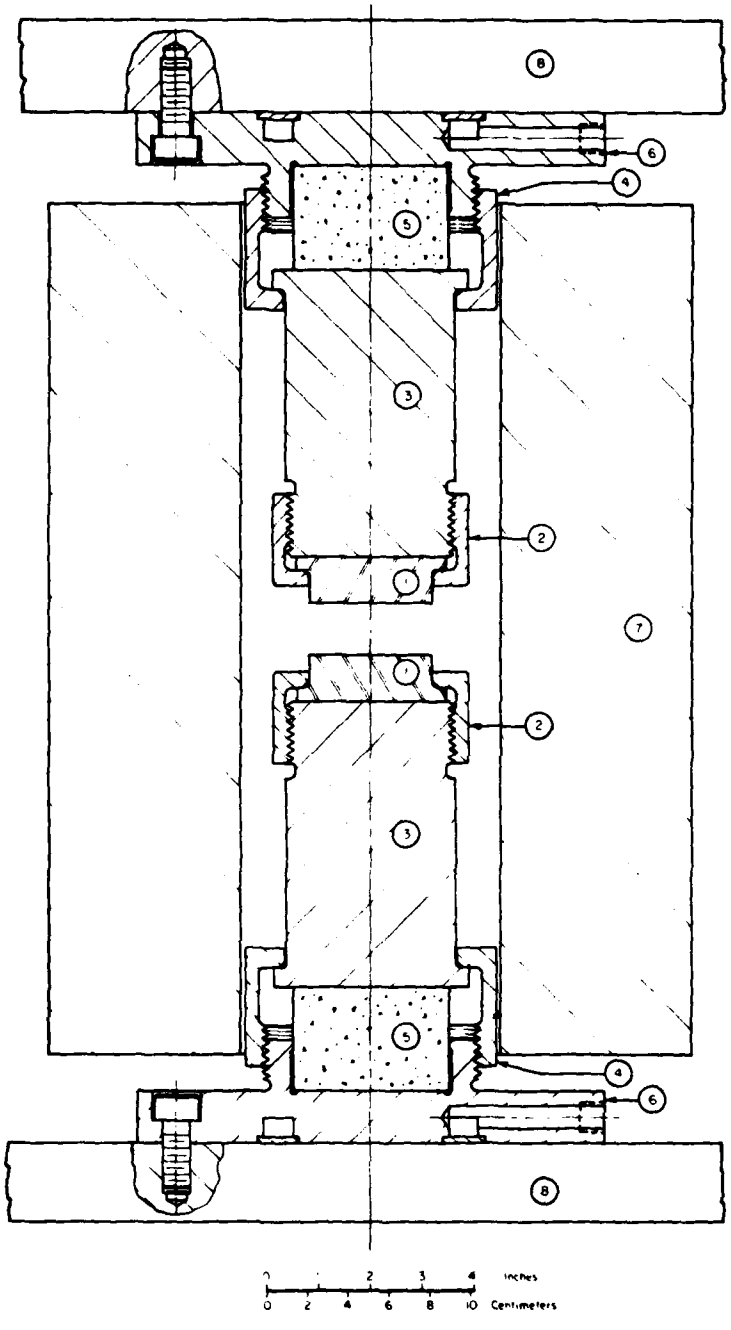

FIGURE 2. Hot-Isothermal Compression Test Fixture. (1 = superalloy compression die, 2 = superalloy die retainer ring, 3 = superalloy die support, 4 = stainless steel support retainer ring 5 = ceramic insulator, 6 = stainless steel compression tool or base , = resistance furnace, 8 = two-post die set.)

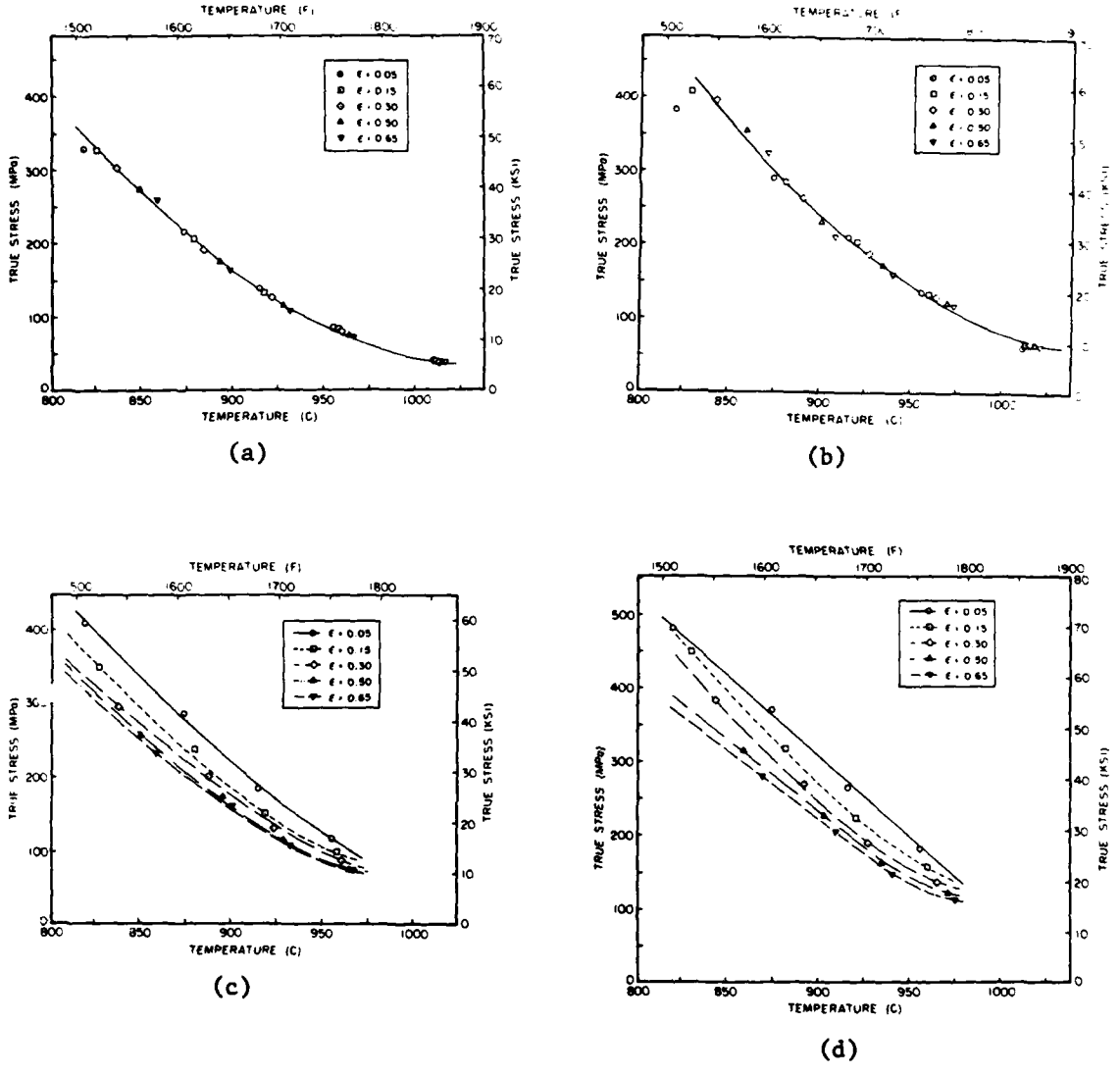

FIGURE 3. Flow Stress as a Function of Temperature after Correction for Adiabatic Heating: (a) α+β Microstructure, $\dot{\varepsilon}$ = 0.1 Sec.$^{-1}$, (b) α+β Microstructure, $\dot{\varepsilon}$ = 1.0 Sec.$^{-1}$, (c) β Microstructure, $\dot{\varepsilon}$ = 0.1 Sec.$^{-1}$, and (d) β Microstructure, $\dot{\varepsilon}$ = 1.0 Sec.$^{-1}$.

on the same trend line except for low temperature-high strain rate combinations. The major conclusion is that a truly isothermal high strain rate hot compression test for this structure would yield a steady state flow stress dependent only on temperature and strain rate, but not strain except at low temperatures and high strain rates where there is still a non-neglibible amount of initial work hardening in the flow curves. The trend lines for the $\alpha+\beta$ structure were used in modeling the deformation and unstable flow behavior to be discussed subsequently.

Sample temperature-corrected data for the β structure are also shown in Figure 3. Whereas adiabatic heating was found to be the major source of the observed flow softening for the $\alpha+\beta$ structure, the "corrected" data for the β structure demonstrated that an additional source of softening exists for the Widmanstatten structure. It is believed that changes in the morphology of the Widmanstatten colonies and a reduction of dislocation density from a high non-equilibrium value in the as-β annealed condition are the source of the additional softening which has also been observed in other HCP metals[3]. Because a technique for quantitatively estimating the level of softening could not be found, modeling of the deformation and unstable flow behavior of β structure was done using sets of trend curves such as those in Figure 3.

The flow stress data in compression were used in obtaining strain rate sensitivity exponents (m in $\sigma = K\dot{\varepsilon}^m$). The values determined were applied in deformation analyses to be discussed subsequently.

Tensile Tests and Thermal Property Characterization

Tensile tests were also run at 816, 913, and 982 C (1500, 1675, and 1800 F) to obtain flow stress data to support the compression flow stress data, which were used in the deformation analyses. These tests were also run in an MTS (at nominal strain rates of 1.5 and 15 per second), and the flow stress data so obtained showed good agreement with the compression flow stress data.

The program materials were also characterized from the standpoint of their thermal properties. To do this, specific heat values were estimated from the published literature and tests, performed under this program, in which the temperature rises caused by deformation heating were actually measured. In

addition, "static" heat transfer experiments in which a hot Ti-6242 sample was placed in contact with room temperature IN-100 dies were performed to obtain values of thermal diffusivity. The thermal properties so obtained were used in the analysis stages of this research program.

Instability Criterion

Torsion Tests

Constant rotation rate torsion tests were run to develop an instability criterion and to establish the occurrence of shear bands in the program alloy under conditions of nominally isothermal, pure shear. To this end, an MTS machine was modified (Figure 4). It was fitted with a hydraulic motor to which was attached an incremental optical encoder which provided closed loop feedback for rotation rate control. In addition, tensile or compressive axial loads could be provided through a linear actuator to counterbalance axial loads which are sometimes produced during torsion as well as to separate specimen halves after fracture. Tubular specimens were induction heated to test temperatures between 816 C (1500 F) and 1010 C (1850 F) and held between specially designed water-cooled grips which allowed rotation.

Similar to the compression results, torsion results showed a marked difference for $\alpha+\beta$ and β microstructures (Figures 5 and 6). The torque-twist curves for β specimens tended to drop off more rapidly than the $\alpha+\beta$ torque-twist curves. Moreover, the uniformity of deformation as evidenced by scribe line measurements was much greater for $\alpha+\beta$ specimens. Shear bands in torsion were indicated by regions in which the angle between the twisting axis and the scribe line were much greater than elsewhere. Such regions were not observed for $\alpha+\beta$ specimens. On the other hand, they were quite prevalent for β specimens, which show marked flow softening in isothermal compression tests. For the β specimens, the scribe line angle ϕ outside the shear band was measured to obtain an estimate of the strain $\bar{\varepsilon}_\ell$ at the onset of the shear localization through the formula $\bar{\varepsilon}_\ell = \gamma/\sqrt{3} = \frac{\tan\phi}{\sqrt{3}}$. Measurements of these strains showed that β torsion specimens went unstable at very small strains [0(0.10)]. These strains are of the same order as the strains at the peaks in the β stress-strain

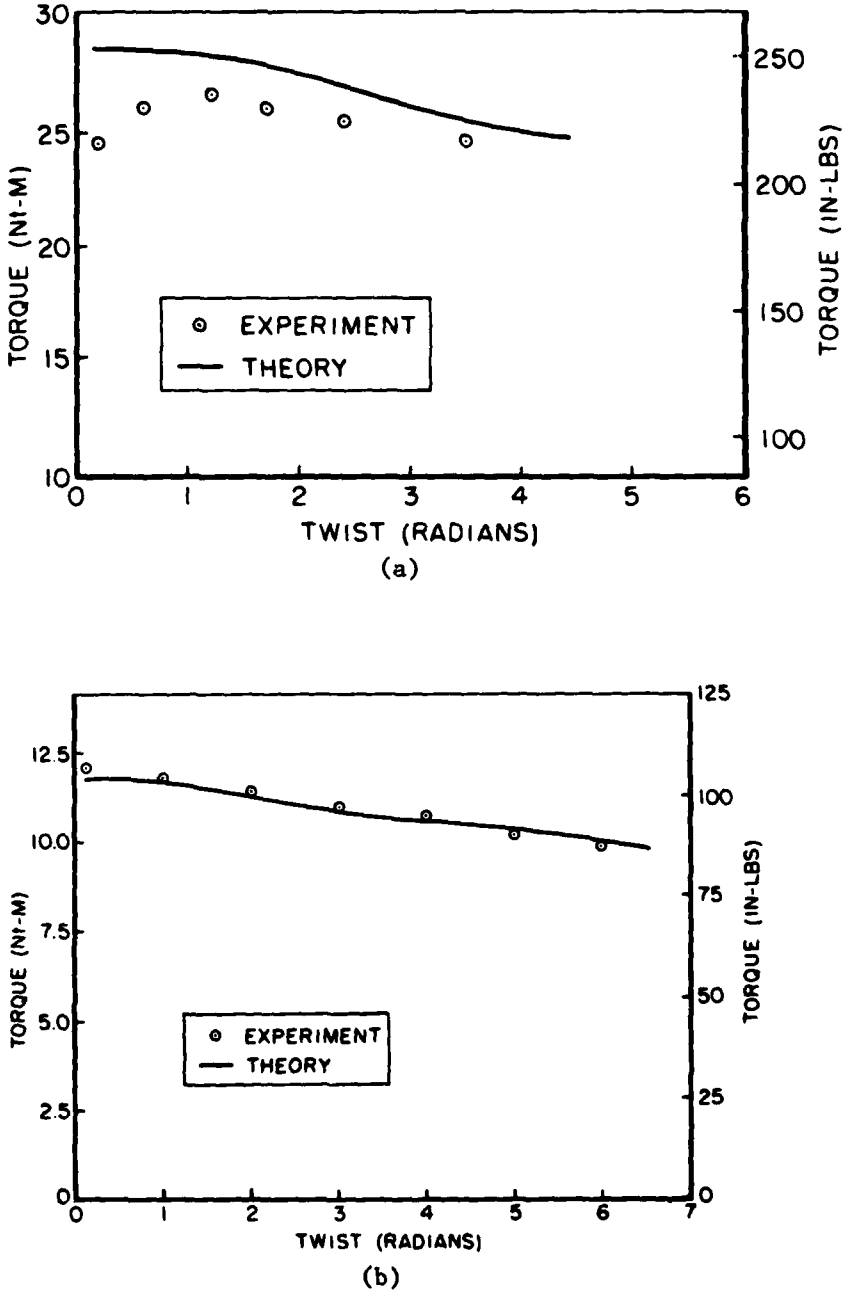

FIGURE 5. Comparison of Experimental and Theoretical Troque-Twist Curves for α+β Microstructure Hot Torsion Specimens Tested at (a) Surface $\dot{\bar{\varepsilon}} \approx 3.3$ Sec.$^{-1}$, T = 816 C (1500 F) and (b) Surface $\dot{\bar{\varepsilon}} \approx 0.9$ Sec.$^{-1}$, T = 913 C (1675 F).

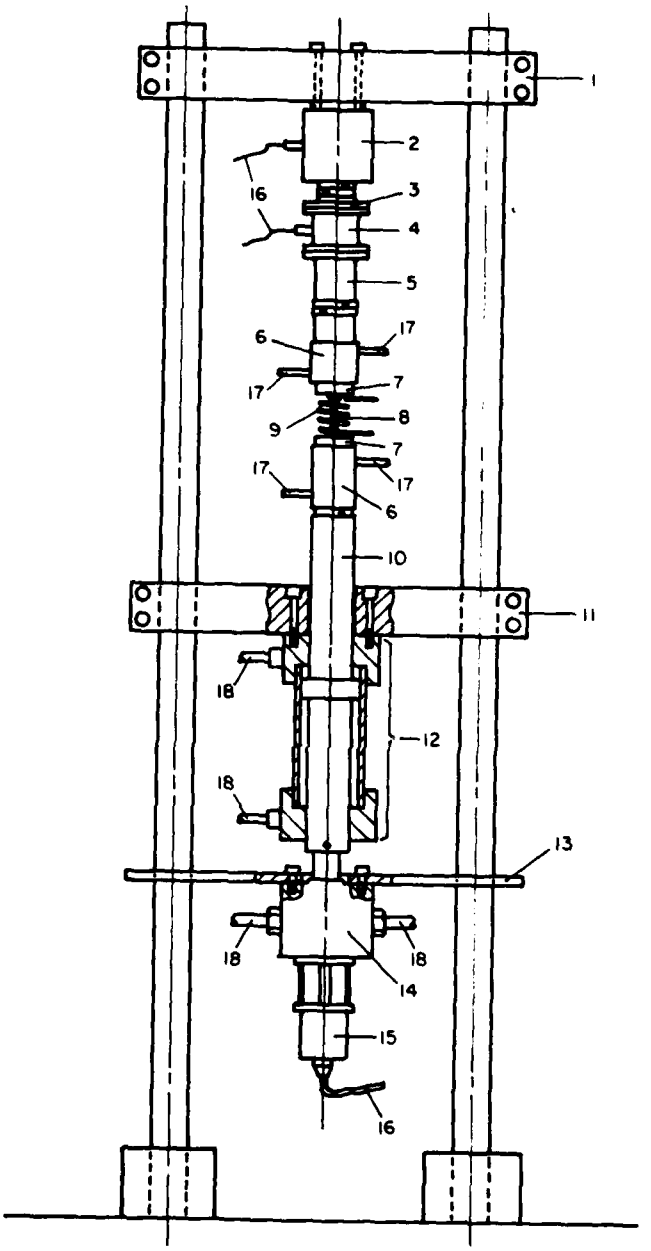

FIGURE 4. MTS Machine Modified for Combined Torsion and Axial Loading. (1 = upper crosshead, 2 = tension load cell, 3 = torque cell adapter #1, 4 = torque cell, 5 = torque cell adapter #2, 6 = water cooled grip, 7 = specimen holder, 8 = specimen, 9 = induction coil, 10 = ram, 11 = lower crosshead, 12 = linear [tension-compression] actuator, 13 = torque reaction plate, 14 = hydraulic motor, 15 = incremental optical encoder, 16 = electrical leads, 17 = water lines, 18 = hydraulic lines)

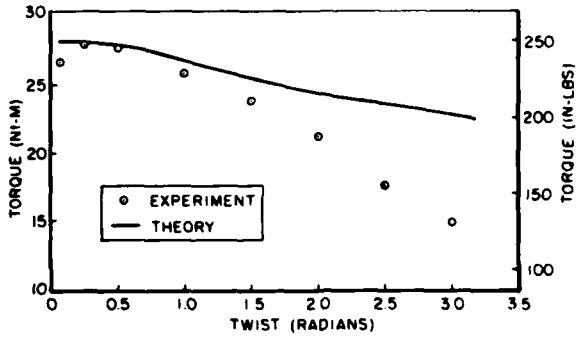

(a)

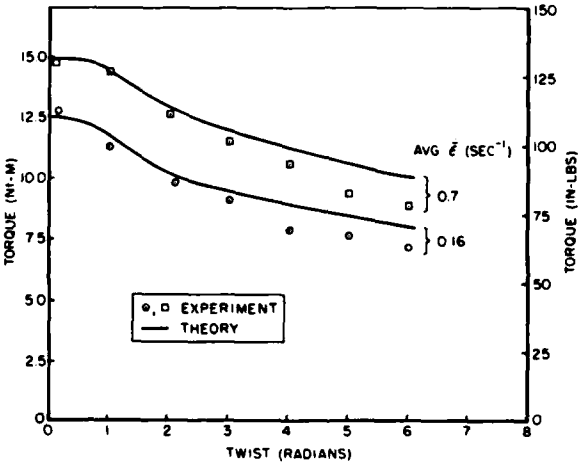

(b)

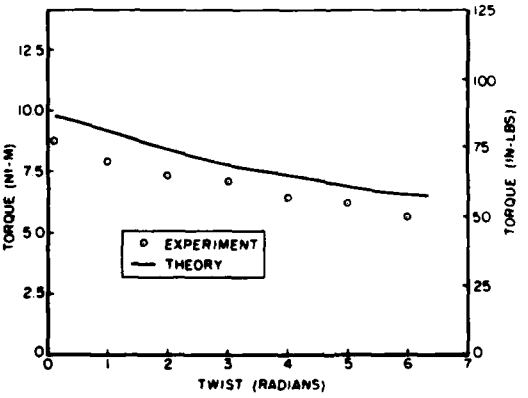

(c)

FIGURE 6. Comparison of Experimental and Theoretical Torque-Twist Curves for β Microstructure Hot Torsion Specimens Tested at (a) Surface $\dot{\bar{\epsilon}} \approx 0.9$ Sec.$^{-1}$, T = 816 C (1500 F), (b) Surface $\dot{\bar{\epsilon}} \approx 0.2$ and 0.9 Sec.$^{-1}$ [Avg. $\dot{\bar{\epsilon}} \approx 0.16$ and 0.7 Sec.$^{-1}$], T = 913 C (1675 F), and (c) Surface $\dot{\bar{\epsilon}} \approx 0.9$, T = 954 C (1750 F).

curves from compression tests. Furthermore, the onset of instability and the development of flow localization in β torsion tests was used to explain why deformation-heat-transfer-analysis predictions were in good agreement with α+β torque-twist curves (Figure 5), but not β torque-twist curves (Figure 6).

Instability/Flow Localization Criterion

In analogy with the tensile instability criterion,[4] it was thought that a necessary condition for torsional instability was a torque maximum, or $dM = 0$. Inspection of the data from the torsion tests revealed that the torque-twist curves of both microstructures and at all temperatures and strain rates used passed through maxima early in the deformation. Hence, additional analysis was needed to explain why only certain of the specimens exhibited true instability and flow localization. This analysis[5] demonstrated that after the torque maximum the rate of twist (or flow) localization, $1/\dot{\theta}\left(\frac{d\dot{\theta}}{d\theta}\right)$, is directly proportional to the "torque softening" rate $\left(= \frac{1}{M}\frac{dM}{d\theta}\right)$, where $M \equiv$ torque, θ = twist, $\dot{\theta}$ = twist rate, and inversely proportional to the strain rate sensitivity.

Parametric studies were done to compare the tendency of the α+β and β microstructures to undergo localized flow in torsion. Using the deformation-heat transfer model, constant twisting rate torsion was simulated on the computer, and torque-twist curves for uniform, stable deformation were generated from hot compression data. Examples of the results for torsion at 913 C (1675 F) are shown in Figure 7. It is obvious from such plots that the β microstructure shows much more "torque softening" than the α+β microstructure. This is reasonable in view of the flow softening trend in hot compression. It is believed that this explains why the β microstructure showed flow localization in torsion at the strain rates and temperatures studied, and the α+β structure did not. The analysis also shows that the localization tendency for the β microstructure is greatest at low strains, which was supported by observation. Lastly, the analysis established the level of the rates of softening which were needed to cause noticeable flow localization (i.e., shear bands) under nominally isothermal hot working conditions. These levels were identical to those found necessary to activate shear bands in isothermal forging, results for which are to be discussed next.

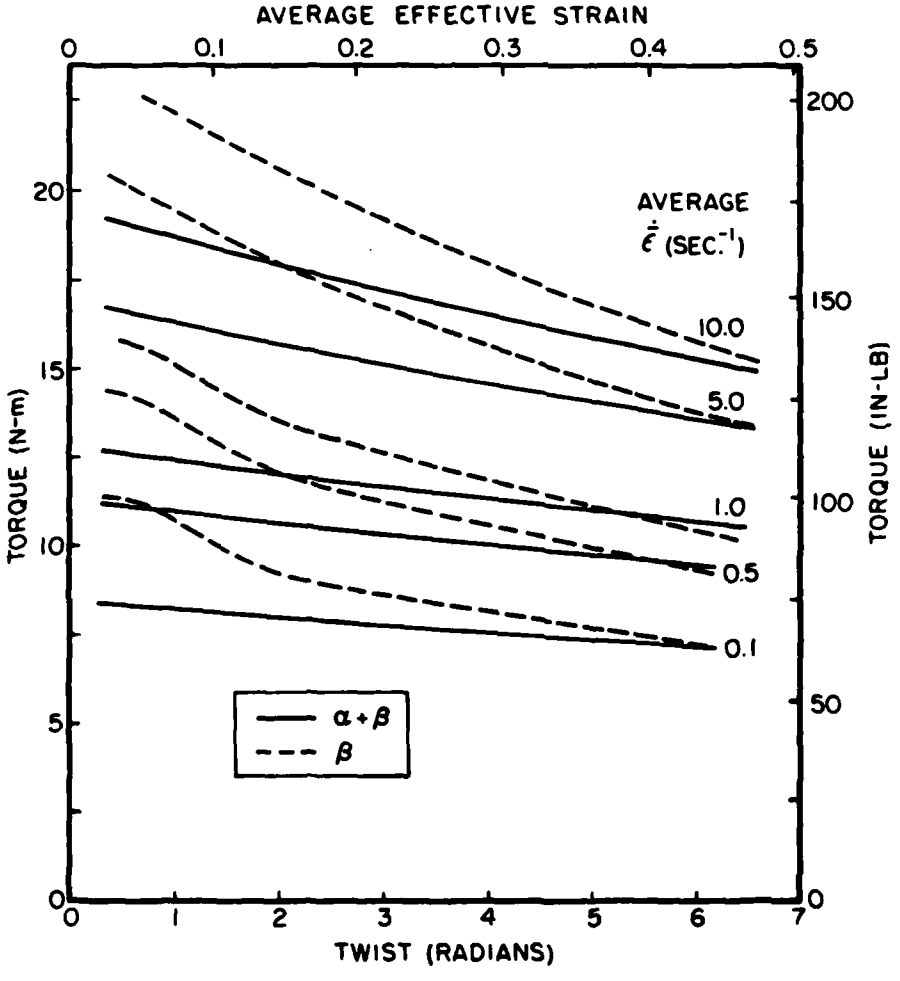

FIGURE 7. Torque Twist Curves Predicted from Numerical Model and Measured Compression Flow Stress Data. Data for Testing at 913 C (1675 F) and Various Average Effective Strain Rates. (Avg. Effective Strain Rate = 0.6 x Surface Effective Strain Rate).

Shear Band Occurrence and Prediction in Isothermal Forging

Shear Band Occurrence

The objective of this phase of the program was to establish the interrelation of mechanics and material behavior on shear band development where temperature gradients are minimal. The objective was achieved by comparing analytical predictions with measurements to establish the effects of strain, strain rate, and temperature on the formation of shear bands in isothermally forged Ti-6242. Isothermal sidepressing was selected as the forging operation because it involves a flow field which appears highly susceptible to shear band formation. Cylindrical specimens measuring 0.71 cm. (0.280 in.) diameter x 2.54 cm. (1.00 in.) long were deformed in an MTS machine at constant crosshead speeds of 0.08, 9.14, and 63.5 mm/sec. (0.0032, 0.36, and 2.5 in./sec.) at temperatures of 843, 913, and 982 C (1550, 1675, and 1800 F). Using the hot, isothermal compression fixture constructed during the first year's program (Figure 2), the specimens were compressed to various levels of deformation to detect shear band initiation.

For $\alpha+\beta$ microstructure sidepressings, shear bands were observed only for the highest deformation rate at the 843 C (1550F) test temperature. In contrast, shear bands in the β microstructure, were observed for all three deformation rates at temperatures of 843 and 913 C (1550 and 1675 F) and for the two higher deformation rates at the test temperature of 982 C (1800 F). In all cases, the shear bands began as regions of intense deformation in the form of X's, the legs of which rotated away from the primary compression axis with increasing deformation. With further deformation, the intersecting shear straining led to the formation of "flat" regions of intense deformation at the center of the specimens, which eventually bowed toward one of the die surfaces with further deformation. Examples of this process for the β microstructure are shown in Figure 8, and a schematic of the overall process is given in Figure 9. A geometric construction was used to obtain an idea of the deformation level at shear band initiation,[6] and it was found that these strains were between 0.3 and 0.5, which corresponded to height reductions (relative to the initial diameter of the sidepressed cylinders) of between 25 and 35 percent.

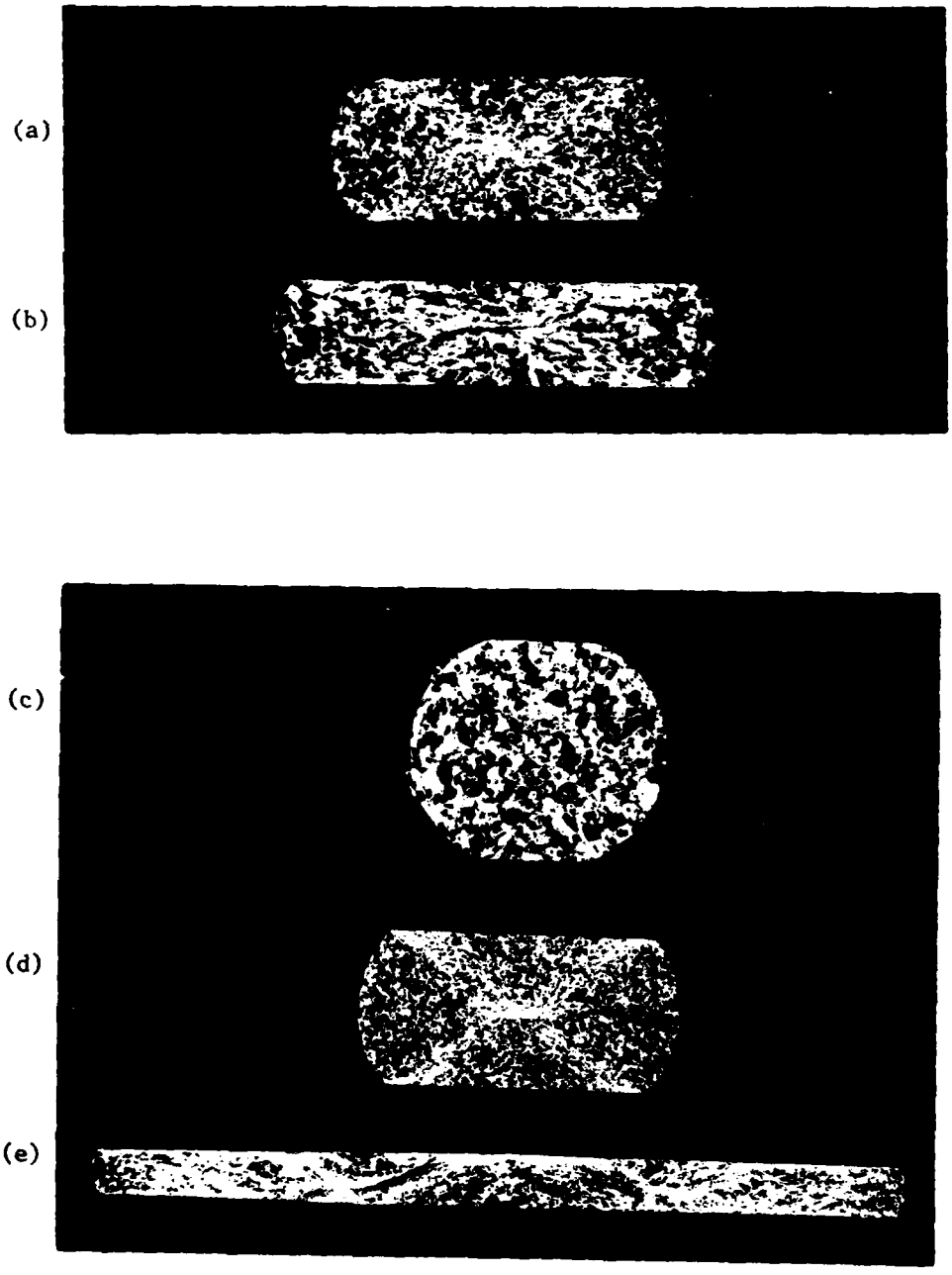

FIGURE 8. Transverse Metallographic Sections of β Microstructure Specimens Isothermally Sidepressed at 843 C (1550 F) Using a Crosshead Speed of (a), (b) 0.08 mm/Sec. (0.0032 In./Sec.) and (c), (d), (e) 63.5 mm/Sec. (2.5 In./Sec.). Reductions are (a) 40%, (b) 59%, (c) 20%, (d) 40%, and (e) 75% (5X)

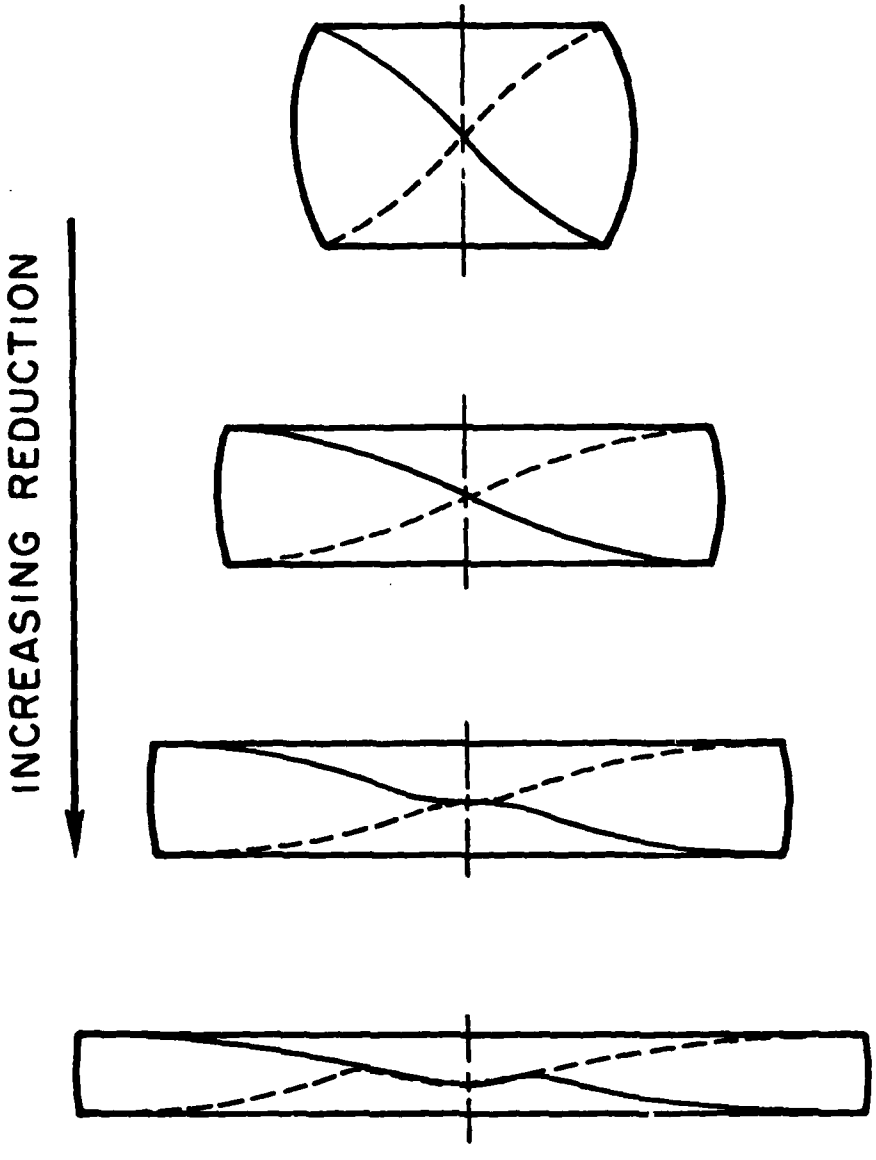

FIGURE 9. Schematic Representation of the Mechanism of Shear Band Formation in Isothermal Sidepressing.

Shear Band Occurrence
Predictions/Workability Maps

The occurrence of shear bands in isothermal forging is strongly dependent on factors such as material properties, geometry, and friction. In all tests, friction was minimal and test geometry was identical. Hence, it is not surprising that the shear bands that were observed followed similar directions in all cases. In fact, these directions are identical to those predicted by slip line field theory.[7] The effect of material properties on the tendency to form flow localizations during isothermal forging has been discussed in a paper based on work from this program.[6] Using an instability criterion, it was shown that the tendency to form flow localizations along directions of maximum shear stress depends on α, the ratio of the non-dimensional work softening rate to the strain-rate-sensitivity parameter.

Jonas, et al.,[8] suggest that materials with α parameters of 5 or greater are particularly susceptible to perisitent flow localizations. The observations for Ti-6242 supported this hypothesis. The α parameters for this material were calculated from flow curves (not corrected for deformation heating) and strain-rate sensitivities measured at various temperatures and strain rates. From these calculations, temperature and strain-rate regimes in which α was equal to or greater than 5 for at least one strain level were determined. This procedrue formed the basis for the development of workability diagrams for the two Ti-6242 microstructures (Figure 10). Analogous to workability diagrams for other kinds of defects found in hot working, these diagrams delineate temperature and strain-rate domains in which shear bands would not be expected (the "SAFE" domains) and domains in which they should be expected ("FAIL" domains). For the most part, the shear band observations supported the theoretical predictions of the workability diagrams (Figure 10). The major discrepancies occurred in observations taken near the bourdaries between the SAFE and FAIL regions and may have been due to the use of α equal to 5 rather than some other value. On the other hand, however, the degree of localization did indeed vary with temperature and strain rate for the β microstructure in the manner suggested by the magnitude of the flow localization parameters.

Application of the α-parameter concept to predict shear band initiation strains was unsuccessful. In contrast, process simulation, using an advanced computer code, worked quite well.

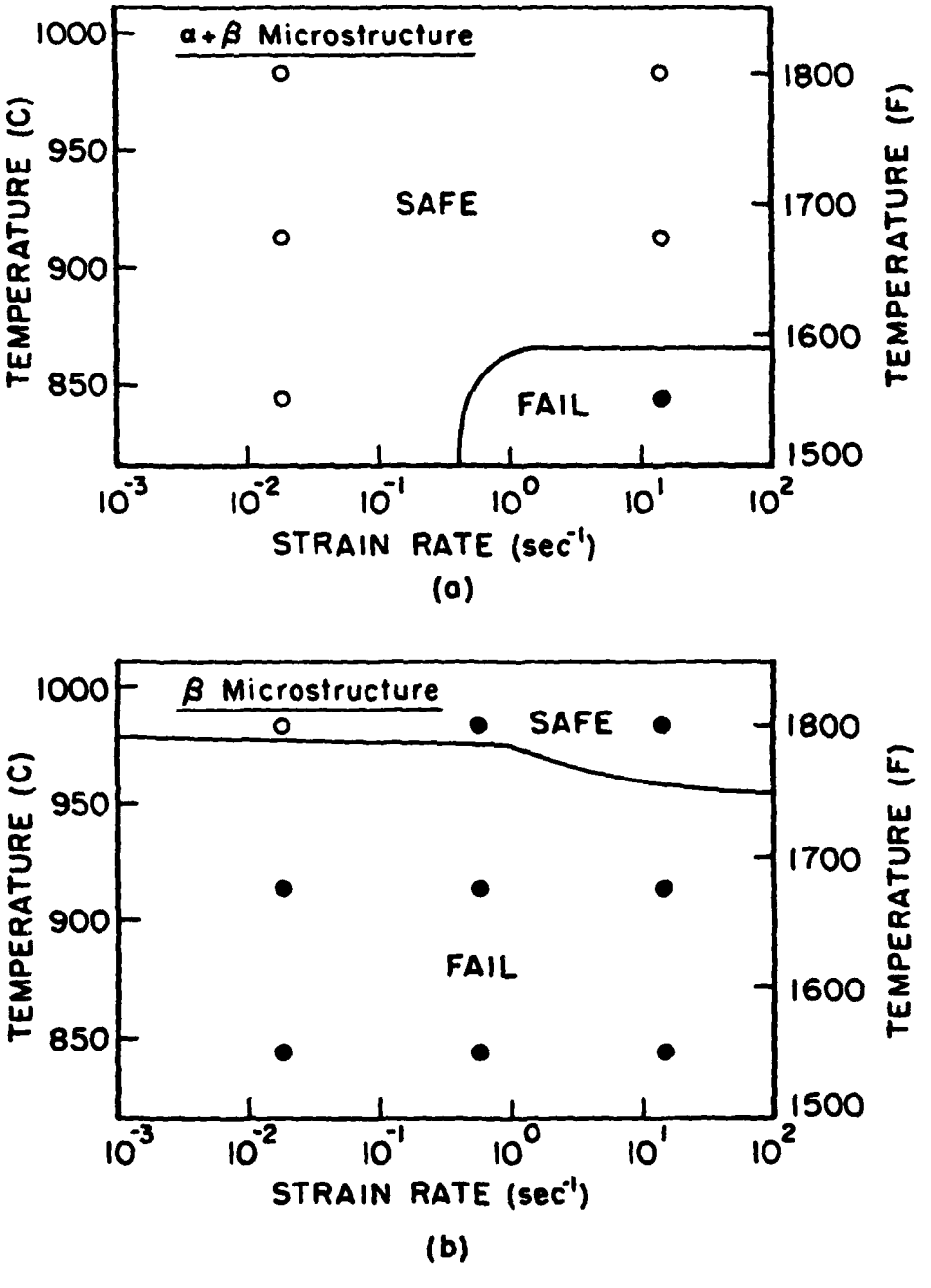

FIGURE 10. Workability Maps for Occurrence of Shear Bands in Hot Forging of Ti-6242 with (a) α+β Microstructure and (b) β Microstructure. Workability Predictions (-) and Forging Conditions in which Shear Bands Were (●) and Were Not (o) Observed are Noted

Shear Band Simulation

Advanced finite element models were applied to simulate the deformation in isothermal sidepressing and thus validate an analytical method for prediction of shear bands in arbitrary forging situations. The general purpose program ALPID developed by Oh[9] was employed for this purpose, and it gave extensive insight into the behavior of metals during isothermal forging.

Isothermal Sidepressing Simulations at 913 C (1675 F). Isothermal sidepressing of specimens of both microstructures was simulated at 913 C (1675 F) and crosshead speeds of 9.14 and 63.5 mm/sec. (0.36 and 2.5 in./sec.) using the program ALPID. From the experimental observations, it was known that these conditions would provide variations in deformation uniformity. The α+β specimens had been found to deform uniformly and the β specimens developed shear bands under these test conditions. Predicted and measured load-stroke curves from all of the simulations agreed well. The excellent correlation suggested that the simulation of the process was accurate.

Insight into the detailed applicability of the simulation was obtained from looking at predicted grid distortions and strain rate fields. Predicted grid distortions in specimens with α+β microstructure deformed at 913 C (1675 F) were not severe even at large reductions, suggesting that the deformation was fairly uniform. This was consistent with the experimental observation. Further, the strain rate contours did not show large gradients across the cross section [Figure 11 for crosshead speed of 9.14 mm/sec. (0.36 in./sec.)]*.

In contrast, the grid distortions in β specimens were considerably non-uniform across the cross section. In addition, the strain rate contours (for example, those in Figure 11) indicated large gradients and the possibility of flow localization along the lines of velocity discontinuity in slip line fields. For the 9.14 mm/sec. crosshead speed, the high strain rate region begins to rotate away from the ordinate at a reduction between 20 and 30 percent (in good agreement with the reduction at which shear bands were observed to initiate experimentally). After 50 percent reduction in height, the

* Because of symmetry considerations, it was only necessary to analyze one-fourth of the cylinder deformation in sidepressing. Hence, deformation and strain rate fields are shown for only the upper right-hand quadrant of the cylinder cross section.

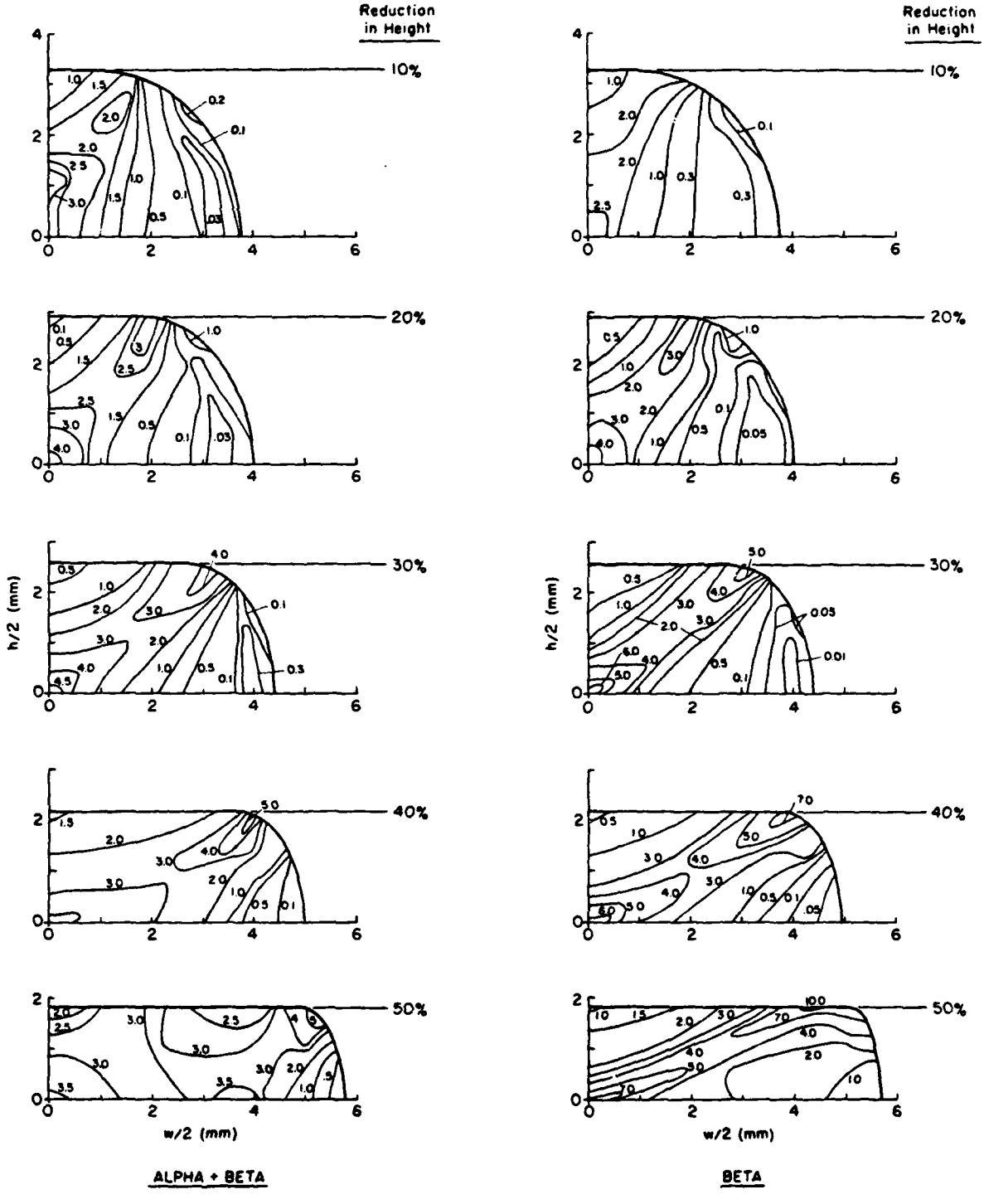

FIGURE 11. Predicted Strain-Rate Contour Plots for Isothermally Sidepressed Ti-6242 with α+β and β Microstructures. Specimen Temperature - 913 C (1675 F), Crosshead Speed - 9.14 mm/sec. (0.36 in./sec.)

predicted deformation pattern became so non-uniform, especially near the center of the specimen, that further computer simulation was not possible without remeshing. At this stage, the predicted strain rate concentration in the β microstructure was twice as high as that in the α+β microstructure. This concentration of strain rate was considered to represent flow localization and formation of shear bands in β material.

Parametric Study of Isothermal Sidepressing. In order to obtain an in-depth idea of the capabilities of the computer code, sidepressing simulations were run from a parametric viewpoint using a wide range of hypothetical material properties typical of hot-forged metals. Most flow stress data in the hot-working regime lie between two extremes (Figure 12). One of these is a flow curve which shows an initial work-hardening interval followed by a flow-stress plateau (Curve A, Figure 12). This curve is typical of much of the α+β microstructure data. The other extreme is a curve, showing little or no initial work-hardening followed by a large amount of flow softening (Curve B, Figure 12), which is typical of much of the β microstructure flow stress data. Strain-rate sensitivity parameters m were set at 0.0, 0.125, or 0.30 in the simulation. With these properties, $\alpha[= -\left(\frac{1}{\sigma}\frac{d\sigma}{d\varepsilon}\Big|_{\dot{\varepsilon}}\right)/m]$ for the hypothetical materials ranged between 0 and ∞, suggesting a wide range of tendencies to form shear bands. In all cases, an arbitrary crosshead speed of 9.14 mm/sec. (0.36 in./sec.) was selected. The crosshead speed was not important because (1) the flow curves had preselected ranges of rate sensitivity m, and (2) the effects of speed and heat transfer on flow properties are implicitly included in the flow curves measured (or postulated) at the constant strain rates in nominally-isothermal-compression tests.

Shown in Figure 13, predicted grid distortions for five different cases show a strong influence of the material properties. For instance, the two cases for which α is less than 5 (Case I, α = 0 and Case II, α = 4.2) exhibit relatively uniform deformation at reductions of 25, 37.5, and 47.5 percent. The simulation of these two cases was taken to 75 percent reduction, with only minor non-uniformities appearing in the second case at reductions greater than 40 percent. For Case III (α undefined), Case IV (α = 10), and Case V (α = ∞), grid distortions are increasingly non-uniform with increasing

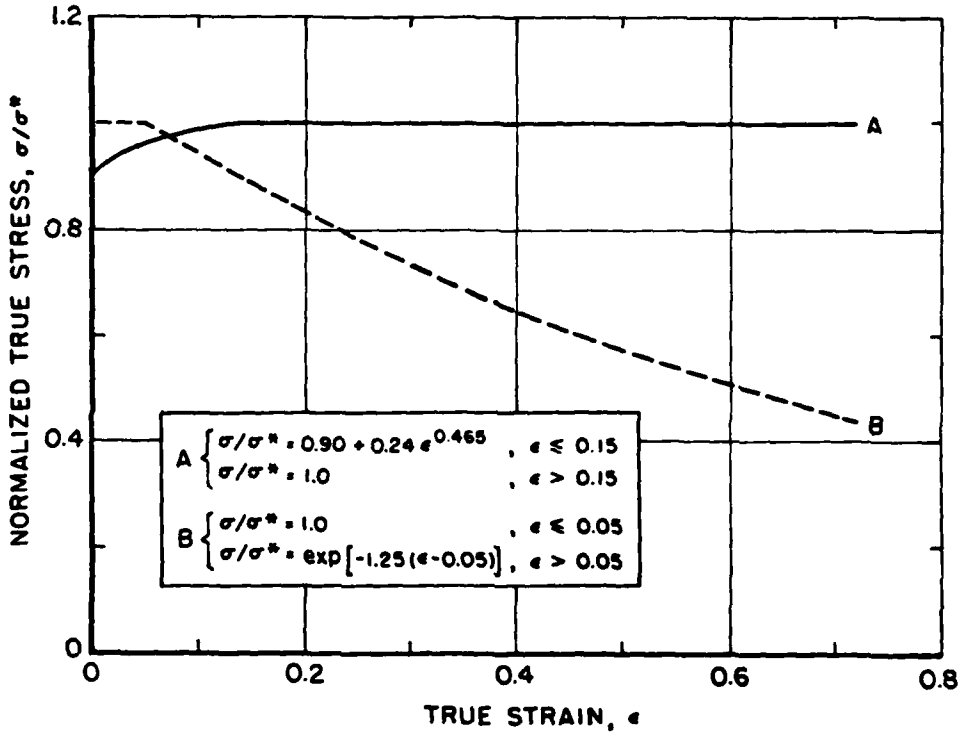

FIGURE 12. Non-Dimensionalized Flow Curves for Metals Deformed in the Hot-Working Regime (Not Corrected for Deformation Heating). Curves Show Extremes of No Flow Softening (Curve A) and Large Amount of Flow Softening (Curve B)

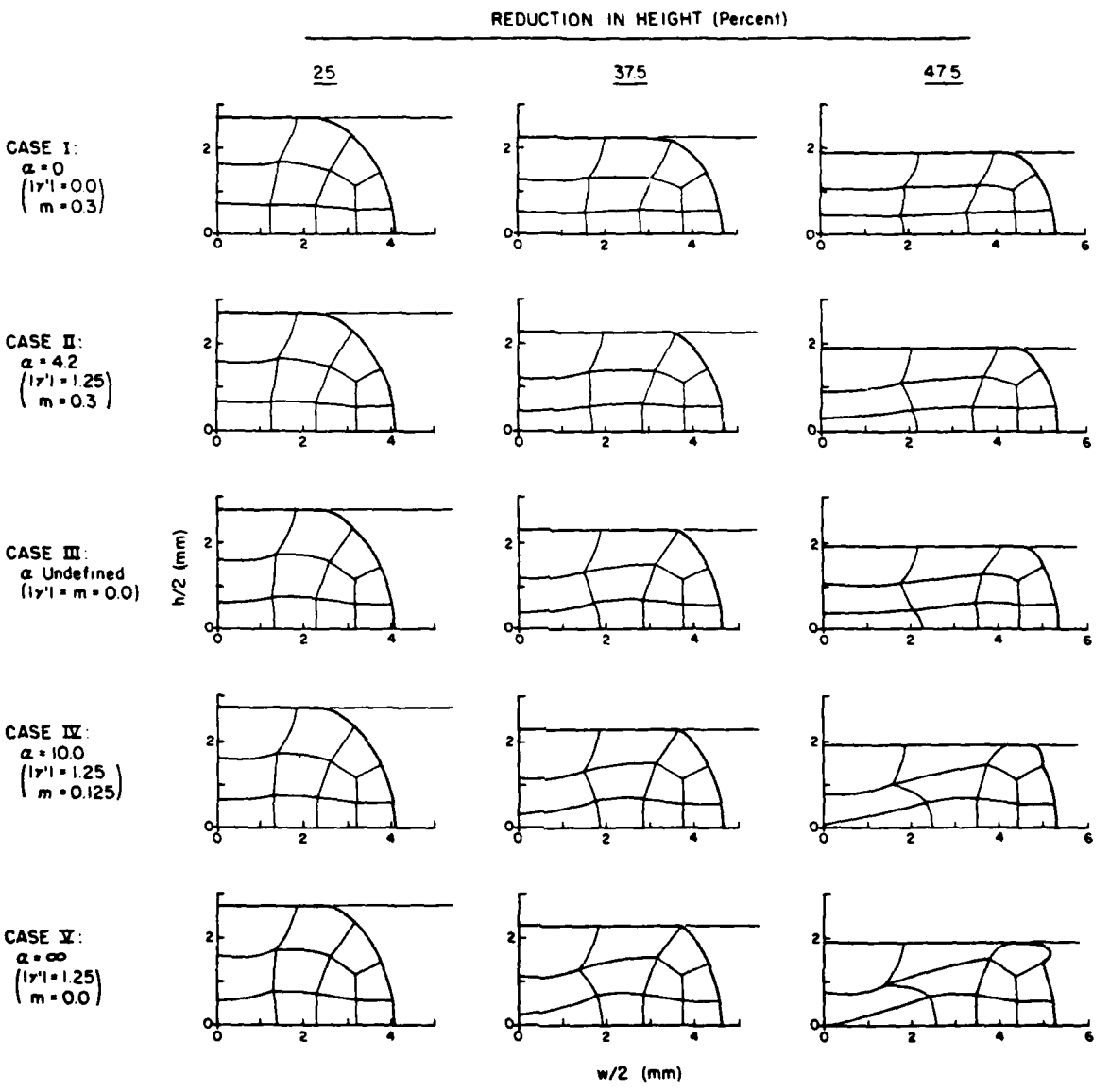

FIGURE 13. Predicted Grid Distortions for Hypothetical Metals with Varying Degrees of Flow Softening ($|\gamma'|$) and Strain-Rate Sensitivity (m)

α at a given reduction, on the one hand, and with increasing reduction for a given α on the other. For Cases IV and V, deformation became so non-uniform after approximately 50 percent reduction that continuation of the simulation was impossible. The grid distortions in Figure 13 also pinpoint the regions of higher-than-average deformation. These may be noted by looking at changes in the angles between intersecting grid lines from which it is observed that deformation is indeed predicted to localize along the directions observed in metallographic sections (Figure 8).

Predicted effective-strain-rate contours (Figure 14) exhibit a trend similar to that for the grid distortions. Strain-rate concentrations increase with increasing α. Modest ones are seen in Cases II and III and strong ones in Cases IV and V. In addition, localizations observed in Cases IV and V occur along lines which rotate toward the abscissa with increasing reduction. For these two cases (and for the others as well), regions of highest strain rate lay at 45 degrees to the ordinate at a reduction of 25 percent. Rotation of these regions occurs at higher reductions. Hence, the initiation event (marked by the reduction at which the angle between intersecting flow localizations deviates from 90 degrees) has been predicted to occur at reductions greater than 25 percent. Another interesting observation is the tendency of the flow localizations to form "flats" near the center of the specimen, much like those actually observed. This can be seen by comparing the 47.5 percent reduction patterns for Cases IV and V to observations in Figure 8. A related phenomenon is seen in Case III, in which the strain-rate localization even moves away from the center. These and other phenomena are highly suggestive of the block shearing required for shear band occurrence. Velocity maps for these cases further confirm and illustrate the physical situation involved in shear band formation and persistence.

Comparison of α Parameter and Simulation Predictions

The simulation results for the wide range of material properties just discussed allow a more complete evaluation of the accuracy of the α-parameter method of predicting shear bands in isothermal forging. As shown by simulation, intense shear bands should definitely be expected when α is

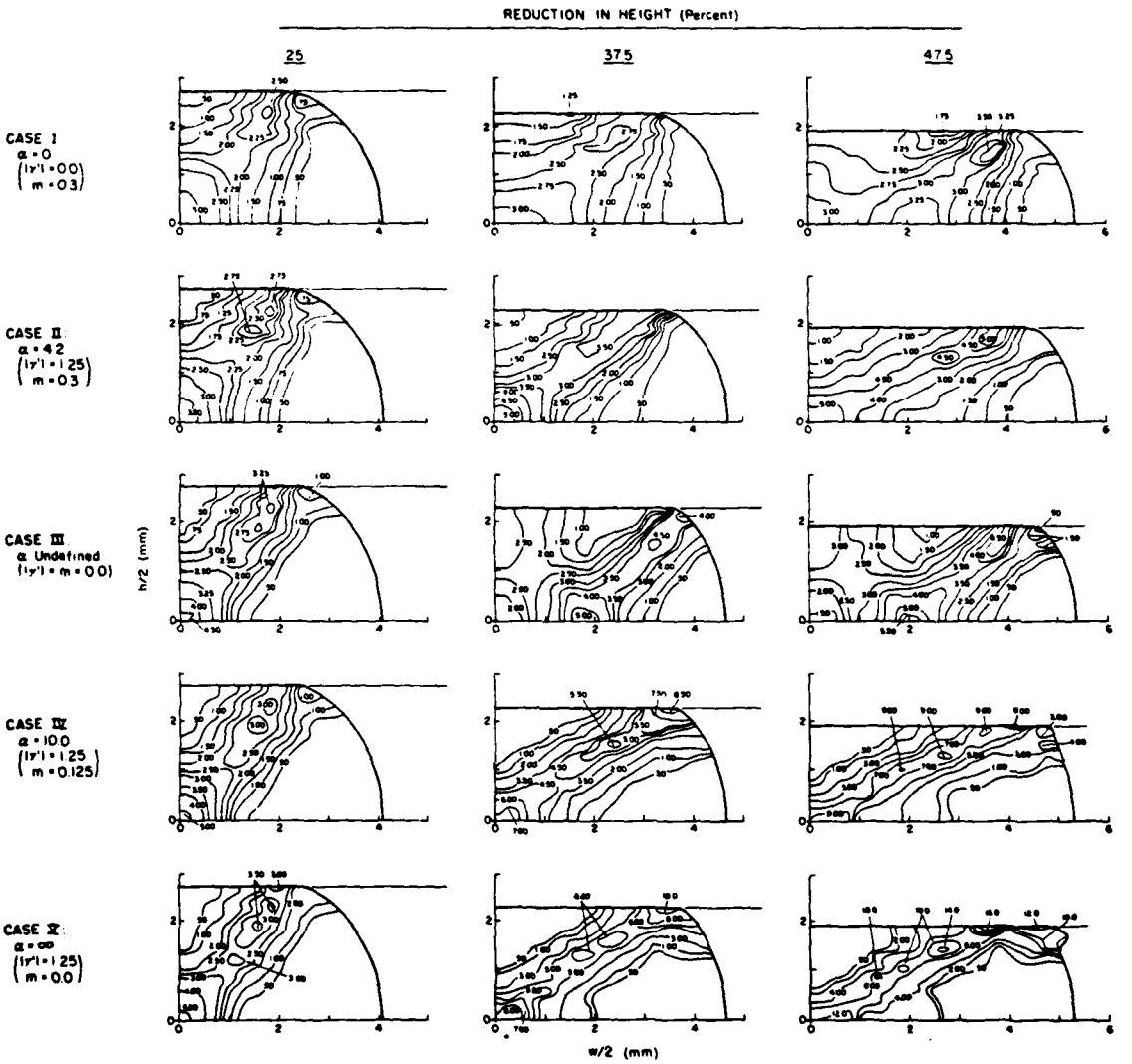

FIGURE 14. Predicted Strain-Rate Contours for Hypothetical Metals with Varying Degrees of Flow Softening ($|\gamma'|$) and Strain-Rate Sensitivity (m)

10 or greater. Furthermore, modest localizations may be expected for α's between 4 and 10. Thus, the use of $\alpha = 5$ as a critical value for shear band occurrence is a useful rule of thumb to obtain a first-order idea of when intense shear bands may be expected. However, it must be kept in mind that it is only approximately valid and that at best it indicates the degree of tendency toward localization, and not the occurrence per se.

Another feature illustrated by the process simulation results is the fact that flow localization is a process and not an event. Strain and strain rate concentrations do not occur instantaneously. For this reason, flow localization cannot be expected to occur when α first reaches some critical value (such as 5) at some point in the flow field. Application of this premise for Cases IV and V, for example, would require flow localization to be noticed at the reduction at which some material element has undergone an effective strain of $\bar{\varepsilon} = 0.05$, which, because of inhomogeneous deformation, should occur at a reduction less than that corresponding to an effective thickness strain of 0.05. Simulation shows though that localizations are first developed at a reduction between 25 and 37.5 percent, which corresponds approximately to effective thickness strains between 0.33 and 0.54 which is in good agreement with observations.

Shear Band Occurrence and Prediction in Non-Isothermal Forging

Results

The generation of shear bands in non-isothermally forged Ti-6242 was documented with the objective of establishing the effects of die chilling on shear band development. This task was an extension of the work on isothermal forging to include heat transfer effects. To this end, 1.02 cm (0.4 in.) diameter, 1.52 cm (0.6 in.) high cylinders of $\alpha+\beta$ and β microstructures were upset in a mechanical press ($\dot{\bar{\varepsilon}} \simeq 10$ sec.$^{-1}$) between dies heated to 204 C (400 F). The cylinders were themselves preheated to temperatures of 913 C (1675 F) or 954 C (1750 F). This work offered insight in the development of shear bands in axisymmetric conventional forging operations. To gain insight into shear band development in plane-strain conventional forging operations, 1.02 cm (0.4 in.) diameter, 10.16 cm (4.0 in.) long

cylindrical preforms of both microstructures were non-isothermally sidepressed in either a mechanical press ($\dot{\varepsilon} \approx 20$ sec.$^{-1}$) or a hydraulic press [$\dot{\varepsilon} = 0$ (1 sec.$^{-1}$)]. Specimens (both lubricated and unlubricated) were preheated to either 913 or 982 C (1675 or 1800 F). They were then forged on dies preheated to either 191 or 343 C (375 or 650 F) after dwell times of 0 or 10 secs. (mechanical press) or 4 or 14 secs. (hydraulic press).

In non-isothermal compression, it was found that early deformation is characterized by the formation of "chill caps". This chilling leads to working loads which are somewhat to much higher than those for isothermal deformation (Figure 15), depending in particular on the amount of chilling and the materials' flow stress dependence on temperature. After the formation of chill caps, a band of localized shear passing through the corners of the specimen develops between the caps and the less highly deformed metal in the rest of the specimen (Figure 16). Metal then begins to "flow" along the shear bands. In particular, the specimen edges fold by shearing along the region of localized deformation, a phenomenon which is very common in cold compression tests with poor lubrication[10]. These observations are helpful in the understanding of shear band formation in more complex hot forging situations. However, it should be noted that the shear bands in non-isothermal compression do not always pass totally through the thickness of the sample. Hence, so-called block shearing does not occur unless a drastic change in deformation mode from axisymmetry to plane strain can be accomplished. This explains why shear localizations are usually more severe in plane-strain modes of deformation as compared to axisymmetric ones. As an aside, it has been noted that when severe shear bands and deformation mode changes do occur in nominally axisymmetric deformation, fracture usually ensues.[11]

Load-stroke curves (Figure 17) and deformation features observed metallographically were similar for the two microstructures when they were non-isothermally sidepressed under identical conditions of working speed, preheat temperature, dwell time, lubrication, and reduction. From metallography, it was seen that shear bands initiated and developed according to the same scheme noted in isothermal sidepressing (Figure 9), indicating the important influence of geometry on development of the defects. They occurred in almost all non-isothermal trials with the severity of localization depending on heat transfer and die chilling (the levels of which are determined by processing conditions).

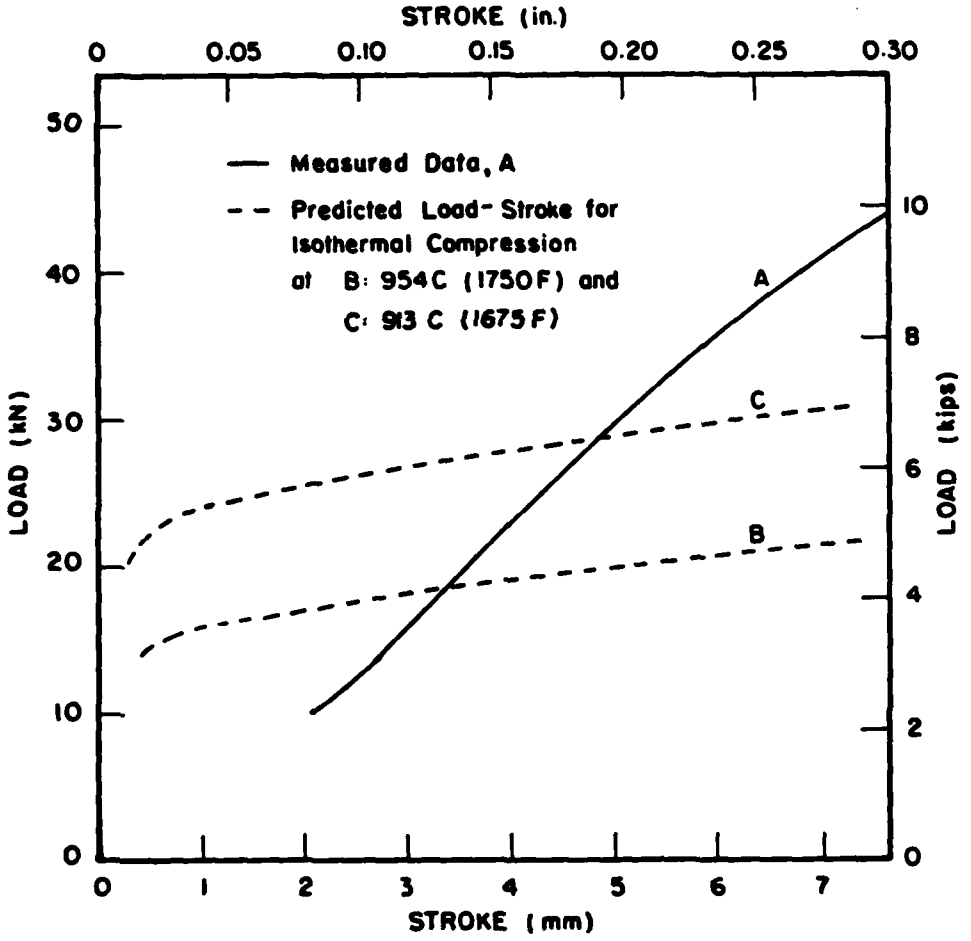

FIGURE 15. Measured Load-Stroke Data (A) for Non-Isothermal Compression of 1.02 cm Diameter, 1.52 cm High α+β Microstructure Sample Preheated to 954 C (1750 F) and Deformed in a Mechanical Press Between Dies Heated to 204 C. Data are Compared to Load-Stroke Curves Predicted for Isothermal Compression at (B) 954 C (1750 F) and (C) 913 C (1675 F).

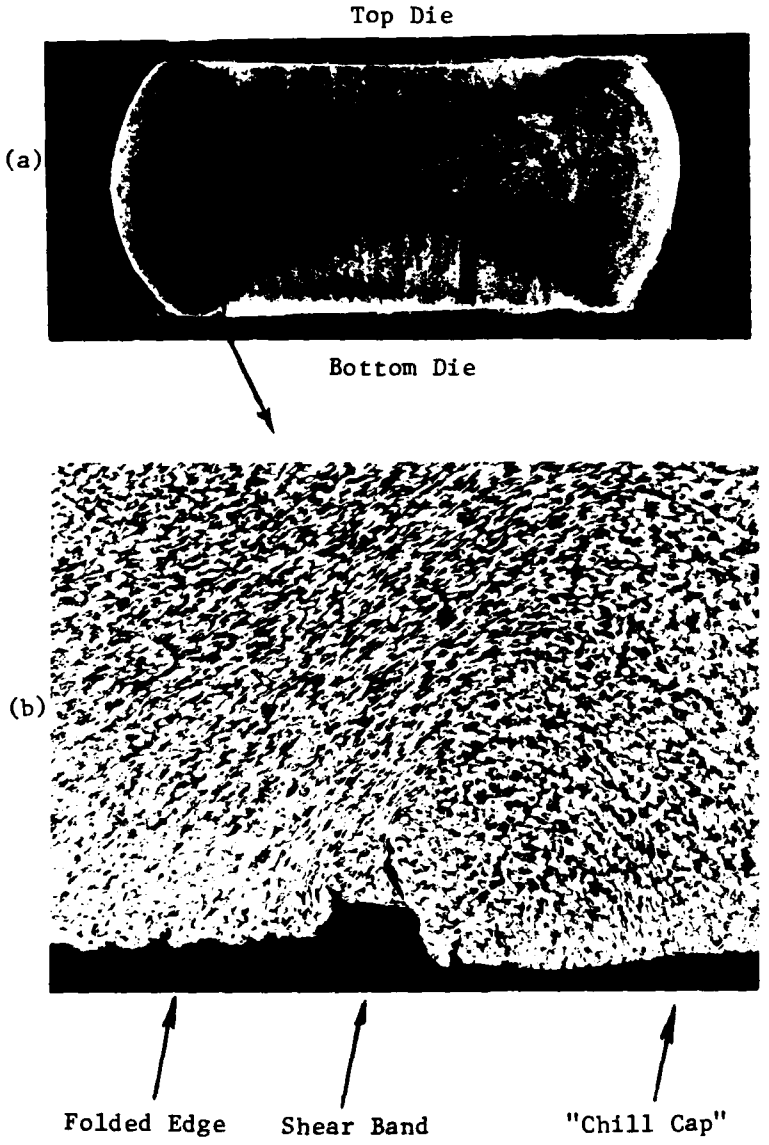

FIGURE 16. 5X Macrograph (a) and 100 X Micrograph (b) of α+β Microstructure Compression Specimen Non-Isothermally Deformed in a Mechanical Press ($\dot{\varepsilon} \simeq 10$ Sec.$^{-1}$). Preheat Temperature 913 C (1675 F), Die Temperature 204 C (400F), Dwell Time 5 Secs.

(a)

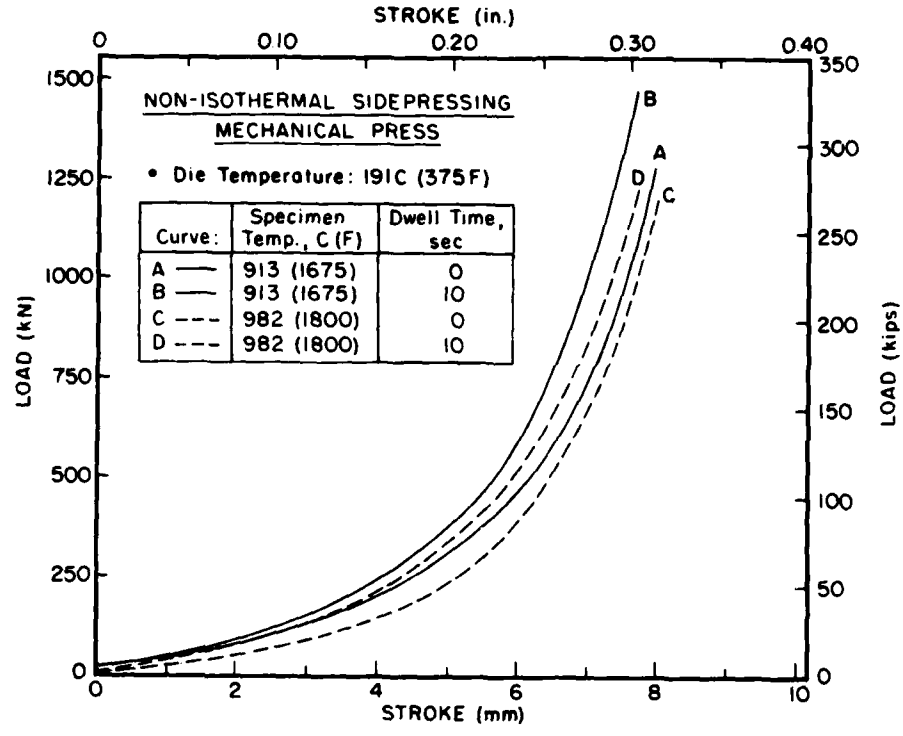

(b)

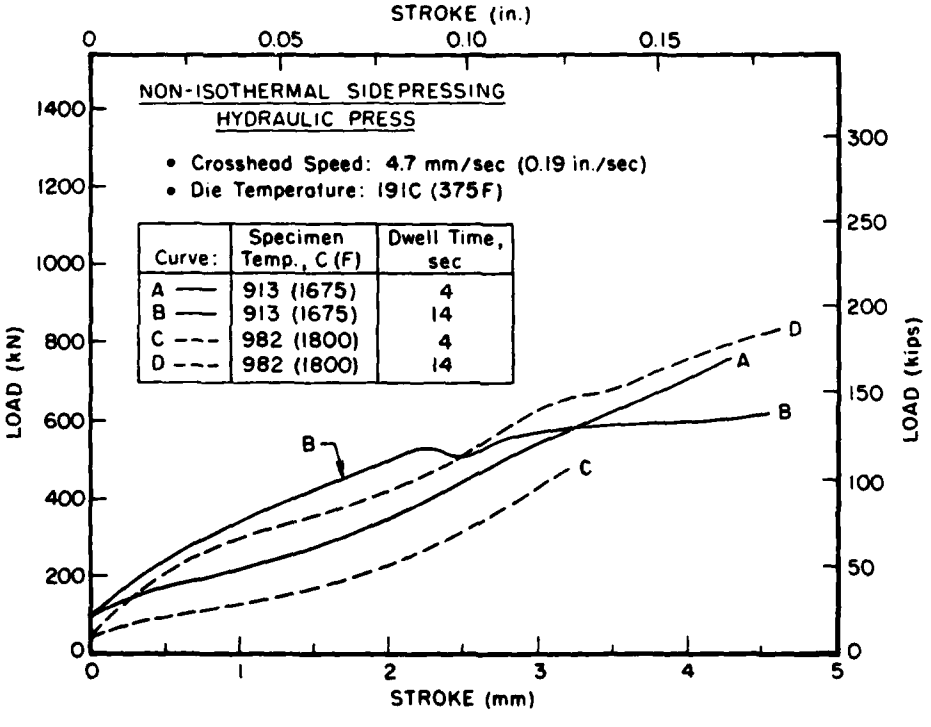

FIGURE 17. Load-Stroke Curves for Non-Isothermal Sidepressing of 1.02 cm (0.40 in.) Diameter, 10.16 cm (4.0 in.) Long Lubricated Preforms of α+β Microstructure in (a) Mechanical Press ($\dot{\varepsilon} \simeq 20$ Sec.$^{-1}$) and (b) Hydraulic Press ($\dot{\varepsilon} \simeq 1$ Sec.^{1}).

For forging in the mechanical press, the degree of localization increased with increasing reductions, lower preheat temperatures, longer dwell times, poorer lubrication, and lower die temperatures, with the first three variables exerting much more of an influence than the last two (Figure 18). Shear band observations from mechanical press forging were similar when bars were sidepressed in blade forging dies (Figure 19). Comparison of these observations with those from the hydraulic press established working speed (through its effect on contact time and heat transfer) as the most important process variable, over the evaluated ranges of speed and dwell time investigated. Not only were the shear bands more intense, they were also the source of many fractures during metalworking in the hydraulic press (Figure 20). Fractures typically occurred at reductions between 30 and 50 percent. This contrasts to results from the mechanical press in which no fractures were observed even at reductions as high as 80 percent.

Discussion of Results

The formation of flow localizations in the form of shear bands in non-isothermal compression and sidepressing is also a manifestation of an instability phenomenon depending on a maximum in stress σ [$(= \sigma(\varepsilon,\dot{\varepsilon},T)$] at some point or points in the flow field. It was found that the development of strain-rate gradients ($d\dot{\varepsilon}/dx$) in the flow field depends on (i) the thermal-softening characteristics ($1/\sigma \frac{\partial\sigma}{\partial T}|_{\dot{\varepsilon},\varepsilon}$) and strain-rate sensitivity (m) of the material and (ii) the imposed thermal gradients $\left(\frac{dT}{\partial x}\right)$ in the workpiece. This dependence was found to be:

$$\frac{d\dot{\varepsilon}/\dot{\varepsilon}}{dx} = - \frac{\frac{1}{\sigma}\frac{\partial\sigma}{\partial T}|_{\varepsilon,\dot{\varepsilon}}}{m} \, dT/dx \quad . \qquad (1)$$

Since the materials terms in this expression are similar for the $\alpha+\beta$ and β microstructures and dT/dx is similar when forging parameters are identical, it is seen that the flow localization tendencies for the two microstructures should be similar. Observation bore this out.

Attempts to simulate the formation of shear bands in non-isothermal forging were made using a modification of the ALPID finite-element program,

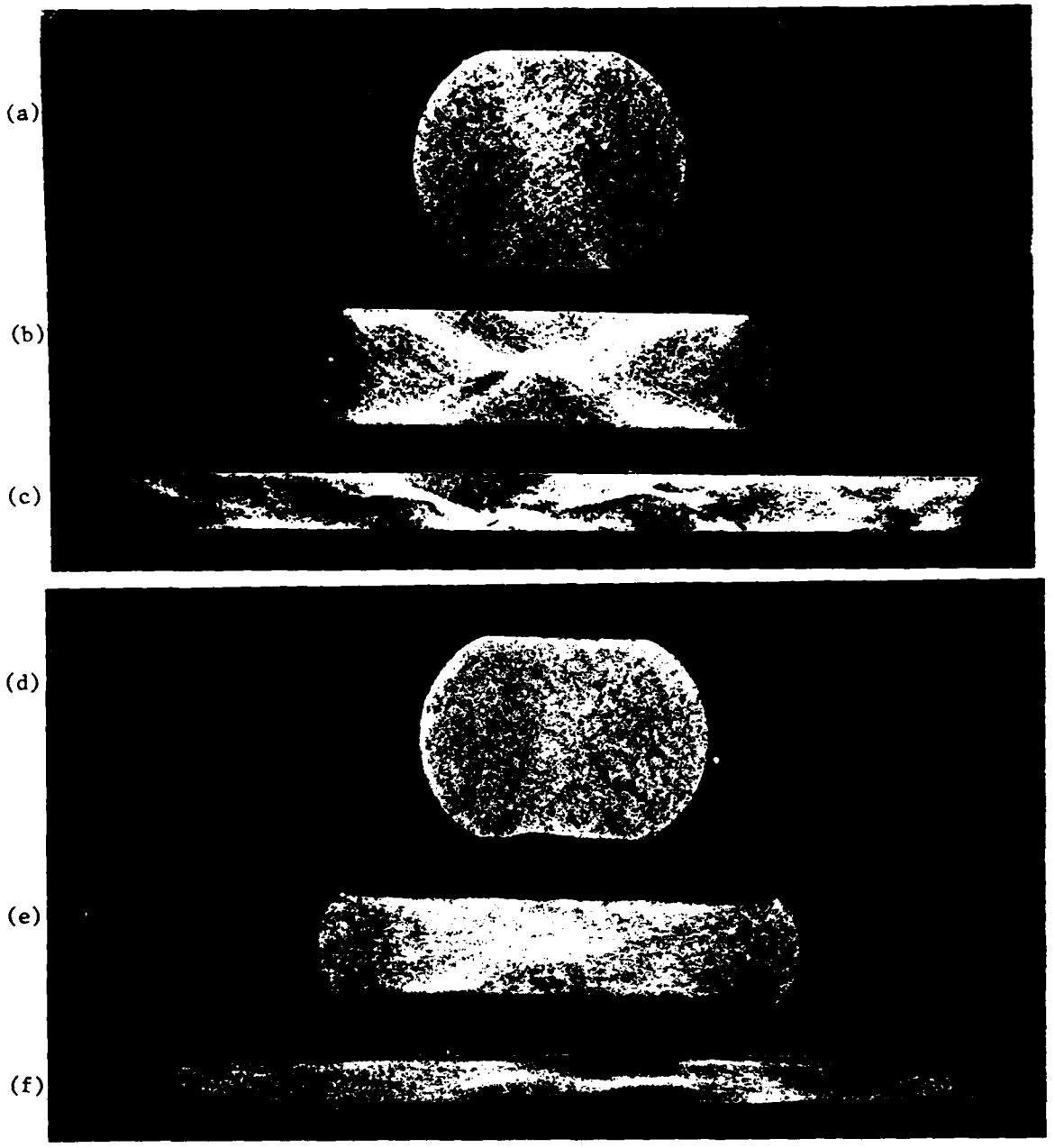

FIGURE 18. Transverse Metallographic Sections of Lubricated α+β Microstructure Specimens Non-Isothermally Sidepressed in a Mechanical Press ($\dot{\varepsilon} \approx 20$ Sec.$^{-1}$). Die Temperature 191 C (375 F), Dwell Time 0 Secs., Specimen Preheat Temperature: (a), (b), (c) 913 C (1675 F), (d), (e), (f) 982 C (1800 F). Reductions are (a) 14 pct., (b) 54 pct., (c) 77 pct., (d) 21 pct., (e) 57 pct., and (f) 79 pct. (4X)

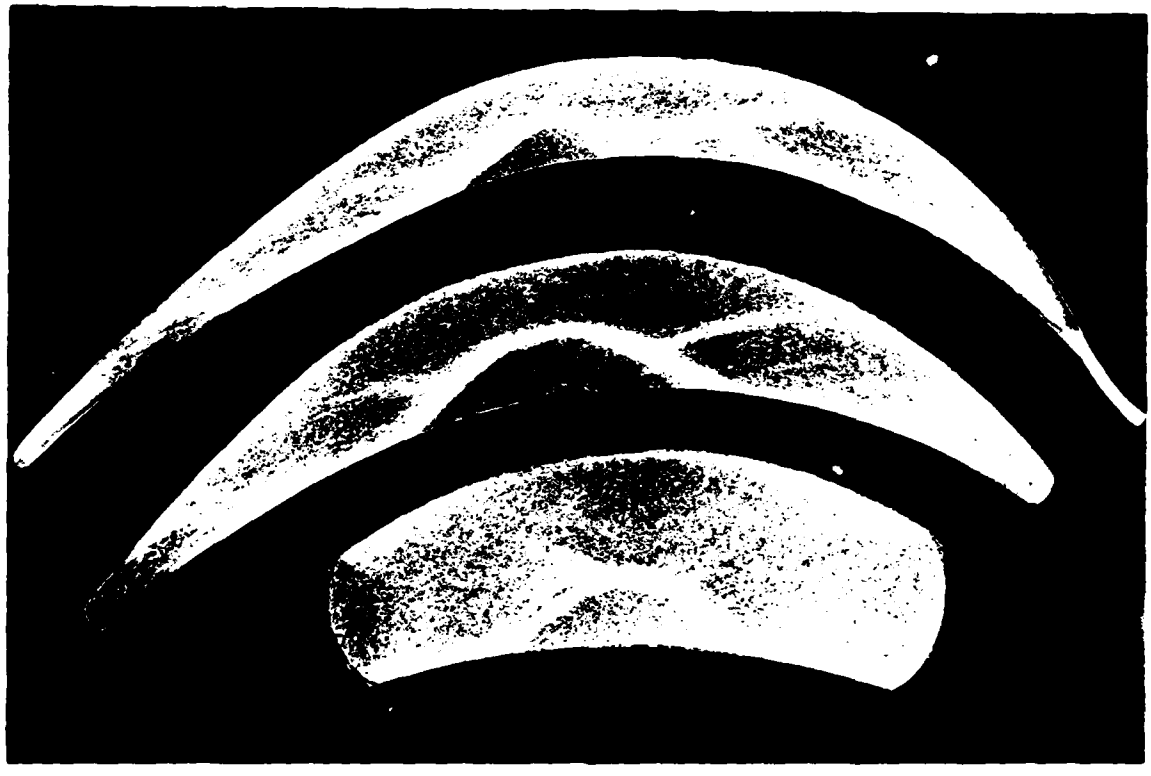

FIGURE 19. Transverse Metallographic Sections from (a) Near End, (b) At Midspan, and (c) Near Root of a Blade Non-Isothermally Forged from a Lubricated $\alpha+\beta$ Microstructure Cylindrical Preform in a Mechanical Press ($\dot{\varepsilon} \approx 20$ Sec.$^{-1}$). Preheat Temperature 913 C (1675 F), Die Temperature 191 C (375 F), Dwell Time 0 Secs. (3-1/2X)

(a)

(b)

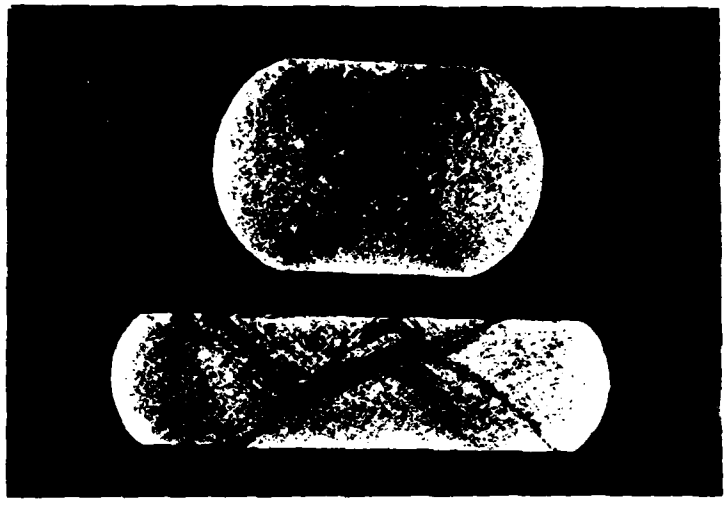

(c)

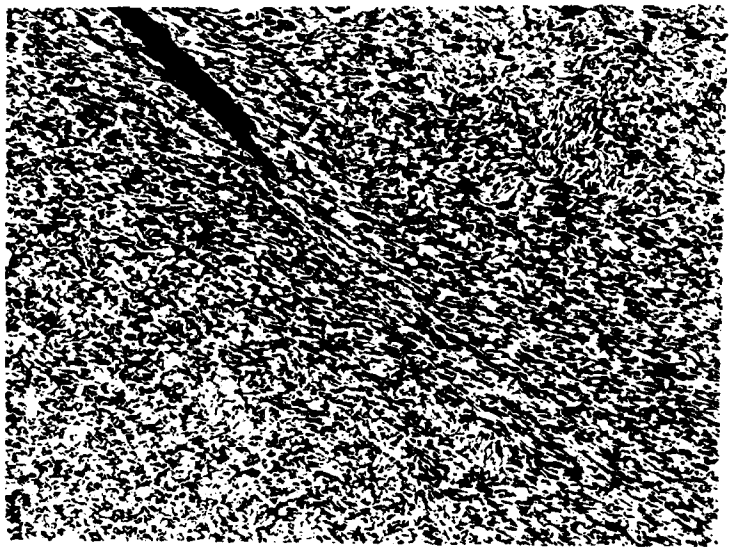

FIGURE 20. (a), (b) Transverse Metallographic Sections (4X) and (c) Micrograph (100X) of Region with Shear Band and Crack from Section Shown in (b) of Lubricated $\alpha+\beta$ Microstructure Specimens Non-Isothermally Sidepressed in a Hydraulic Press ($\dot{\bar{\varepsilon}} \approx 1$ Sec.$^{-1}$). Preheat Temperature 913 C (1675 F), Die Temperature 191 C (375 F), Dwell Time 14 Secs. Reductions are (a) 25% and (b) 53%

which takes into account heat generation and heat transfer effects. These attempts were not successful. An alternate analytical technique, the upper-bound-method, in which a heat transfer analysis was included,[12] was therefore employed to interpret the experimental results. Although detailed strain and strain-rate information could not be gained from this kind of analysis, it gave insight temperature gradients and load behaviors that could be expected.

The upper-bound analysis, which was written for axisymmetric deformations, was applied to the problem of simple compression of $\alpha+\beta$ microstructure, Ti-6242 cylinders (measuring 7 mm (0.28 in.) diameter and 10 mm (0.39 in.) high) deformed in either a hydraulic press ($\dot{\varepsilon} \simeq 1$ sec.$^{-1}$) or a mechanical press ($\dot{\varepsilon} \simeq 20$ sec.$^{-1}$). Analytical results showed that very large temperature gradients are set up in hydraulic press deformations as compared to mechanical press deformations (Figure 21). Thus, in view of the large temperature sensitivity of the flow stress (Figure 3) and Equation (1), it is not surprising that observed shear bands were much more severe in hydraulic press forging (Figures 18, 20). Moreover, the generally lower temperatures experienced during hydraulic press forging, as predicted in Figure 21, probably explain the fracture phenomena observed in sidepressing since it has been found that the workability of Ti-6242 drops off greatly below 816 C (1500 F).[13]

Inspection of the predicted temperature magnitudes (Figure 21) and the flow stress dependence on temperature also explains why forging loads were predicted (Figure 22) to be substantially higher in hydraulic press forging, despite the slower deformation rate. This trend is similar to that for the sidepressing results shown in Figure 17, which incidentally also show unusual inflection points in the hydraulic press load-stroke behavior similar to those predicted for hydraulic press non-isothermal compression in Figure 22.

Effect of Shear Bands on Service Properties

The bulk of the research in the final year of the program concentrated on establishing the effects of shear bands in hot-forging of Ti-6242 on mechanical properties in tension, creep, and fatigue. This was thought to be an important area of investigation since others have found degradation of mechanical properties resulting from the presence of shear bands. For example,

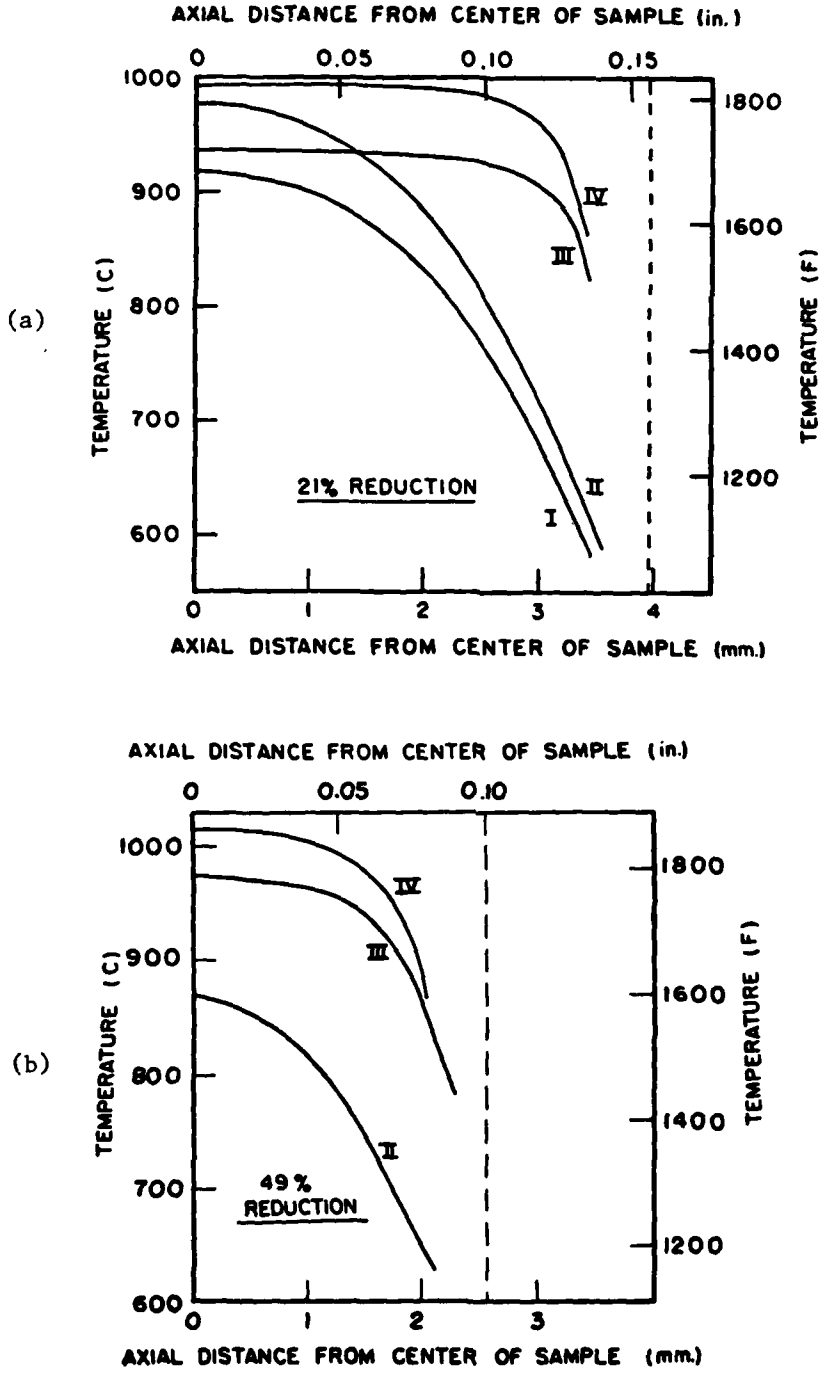

FIGURE 21. Predicted Symmetry Axis Temperature Profiles for (a) 21 pct. and (b) 49 pct. Reduction in Height. Cases I and II are for Compression in Hydraulic Press ($\dot{\varepsilon} \approx 1$ Sec.$^{-1}$). Cases III and IV are for Compression in Mechanical Press ($\dot{\varepsilon} \approx 20$ Sec.$^{-1}$). Specimen Preheat Temperatures were 913 C (Case I and III) or 982 C (Cases II and IV). Dies were Assumed to be Heated to 190 C Initially.

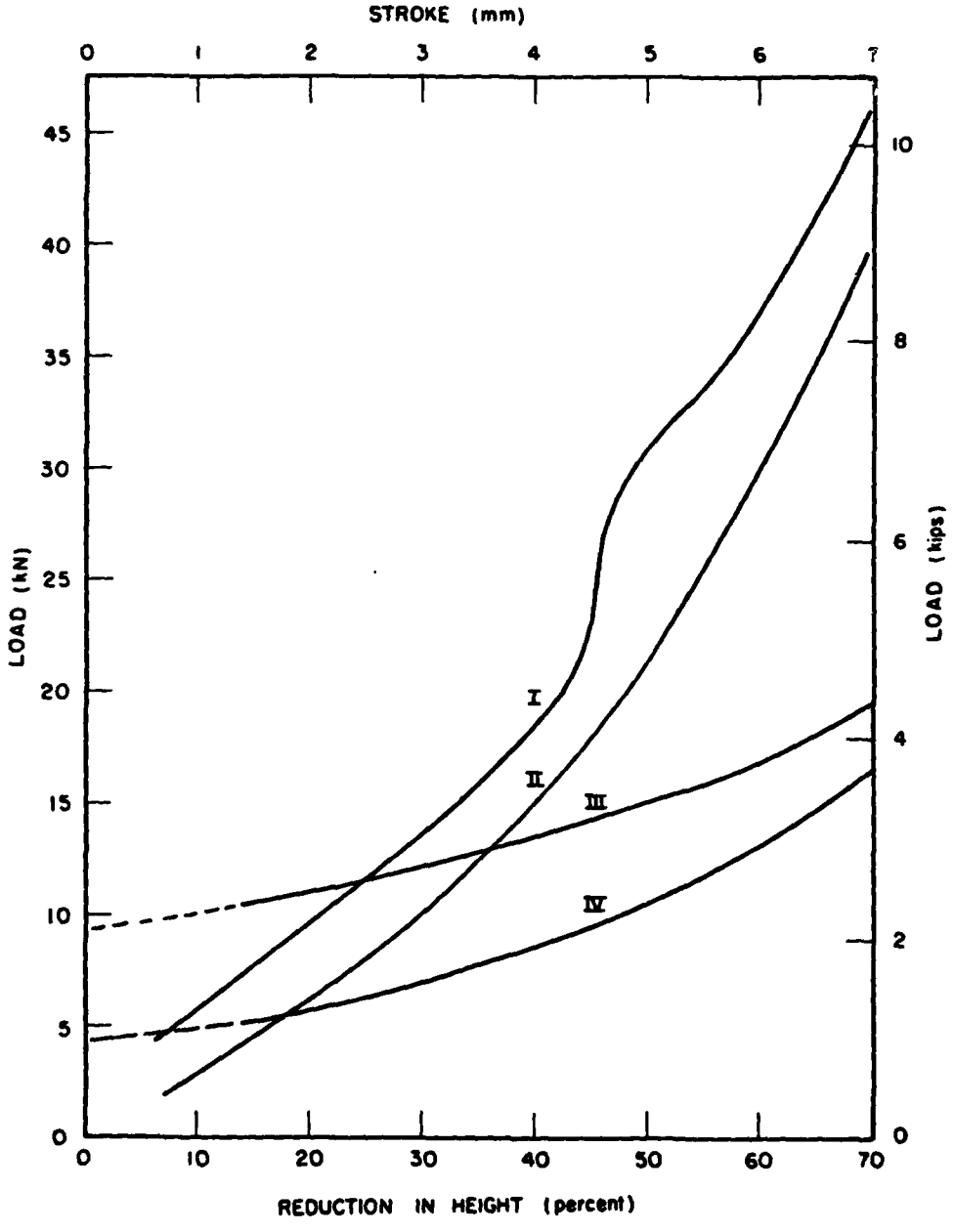

FIGURE 22. Predicted Load-Reduction Curves for Non-Isothermal Compression Cases I, II Hydraulic Press ($\dot{\varepsilon} \approx 1$ Sec.$^{-1}$) and Cases III,IV Mechanical Press ($\dot{\varepsilon} \approx 20$ Sec.$^{-1}$). Specimen Preheat Temperatures were 913 C (Cases I and III) or 982 C (Cases II and IV). Dies were Assumed to be Heated to 190 C Initially.

Pepe has noted that shear bands developed in hydrostatic extrusion of various ferrous, magnesium, and aluminum alloys can severely limit subsequent performance under tensile loading.[14,15]

Generations of Shear Bands under Controlled Conditions and Effect of Heat Treatment on Shear Bands

Under this phase, 1.52 cm (0.6 in.) diameter, 7.62 cm (3.0. in.) long bars of Ti-6242 of $\alpha+\beta$ and β microstructures were forged (i.e., sidepressed) in a mechanical press ($\dot{\varepsilon} \approx 20$ sec.$^{-1}$) to determine conditions which lead to shear banding and conditions in which shear banding is avoided. Previous experimental work was helpful in selecting a range of forging temperatures, die temperatures, and dwell times to obtain forged microstructures with and without shear bands (Table 1). In addition, the just-discussed-process-simulation results on non-isothermal forging which were completed under this task, gave insight into the severity of the flow localizations to be expected in hot-forged Ti-6242 samples. For example, process simulation results suggested that raising the preheat temperature of $\alpha+\beta$ or β preform microstructure samples to just below the transus temperature (~ 988 C (1810 F)) was effective in keeping the sample temperature during forging out of the regime in which the flow stress is most sensitive to temperature, i.e., out of the regime in which shear banding is most severe (Figure 21).

After forging, samples were heat treated to determine the effect of post-forging heat treatment on shear band morphology. Samples were solution-annealed over a range of temperatures between 899 and 1010 C (1650 to 1850 F) and then aged for 8 hours at 593 C (1100 F). The solution treatment temperatures span those commonly used commercially, and the aging treatment is typical for the Ti-6242 alloy which contains 0.1 Si. Following heat treatment, it was found that only beta solution annealing could totally eliminate evidence of shear bands (Table 1, Figures 23 and 24). The other heat treatments, although not totally eliminating the shear bands, had a tendency to "diffuse" or make less severe the localized irregularities in the microstructure caused by the development of shear bands in hot-forging. This was especially evident for heat treatments involving higher temperature, subtransus solution annealing.

TABLE 1. Processing Conditions Evaluated for Development of Shear Bands

Preform Microstructure	Forging Temp. (C)	Die Temp. (C)	Dwell Time (secs.)	Shear Band Rating+ for Heat Treatment Code±: F	A	B	C	D
α+β	913	191	0.	1	1.5	2	3	3
α+β	913	191	10.	1	1*	2*	2.5	3
α+β	913	371	0.	1	1	2	2.75	3
α+β	982	191	0.	3	3	3	3	3
α+β	982	191	10.	3	3	3*	3	3
α+β	982	371	0.	3	3	3*	3	3
β	913	191	0.	1	2.25	2.25	2.25	3
β	913	191	10.	1	1.75*	2*	2	3
β	913	371	0.	1	2.75	2.75	2.75	3
β	982	191	0.	3	3	3	3	3
β	982	191	10.	2.5	3	3*	3	3
β	982	371	0.	3	3	3*	3	3

+ Qualitative Shear Band Rating System:
  1 - Intense Shear Bands
  2 - Weak Shear Bands
  3 - No Shear Bands

* Processing Conditions Used to Make Samples for Mechanical Property Evaluation

± Heat Treatment Codes:
  F : As-Forged (No Heat Treatment)
  A : 899 C/1 Hr. + 593 C/8 Hrs.
  B : 954 C/1 Hr. + 593 C/8 Hrs.
  C : 979 C/1 Hr. + 593 C/8 Hrs.
  D : 1010 C/1 Hr. + 593 C/8 Hrs.

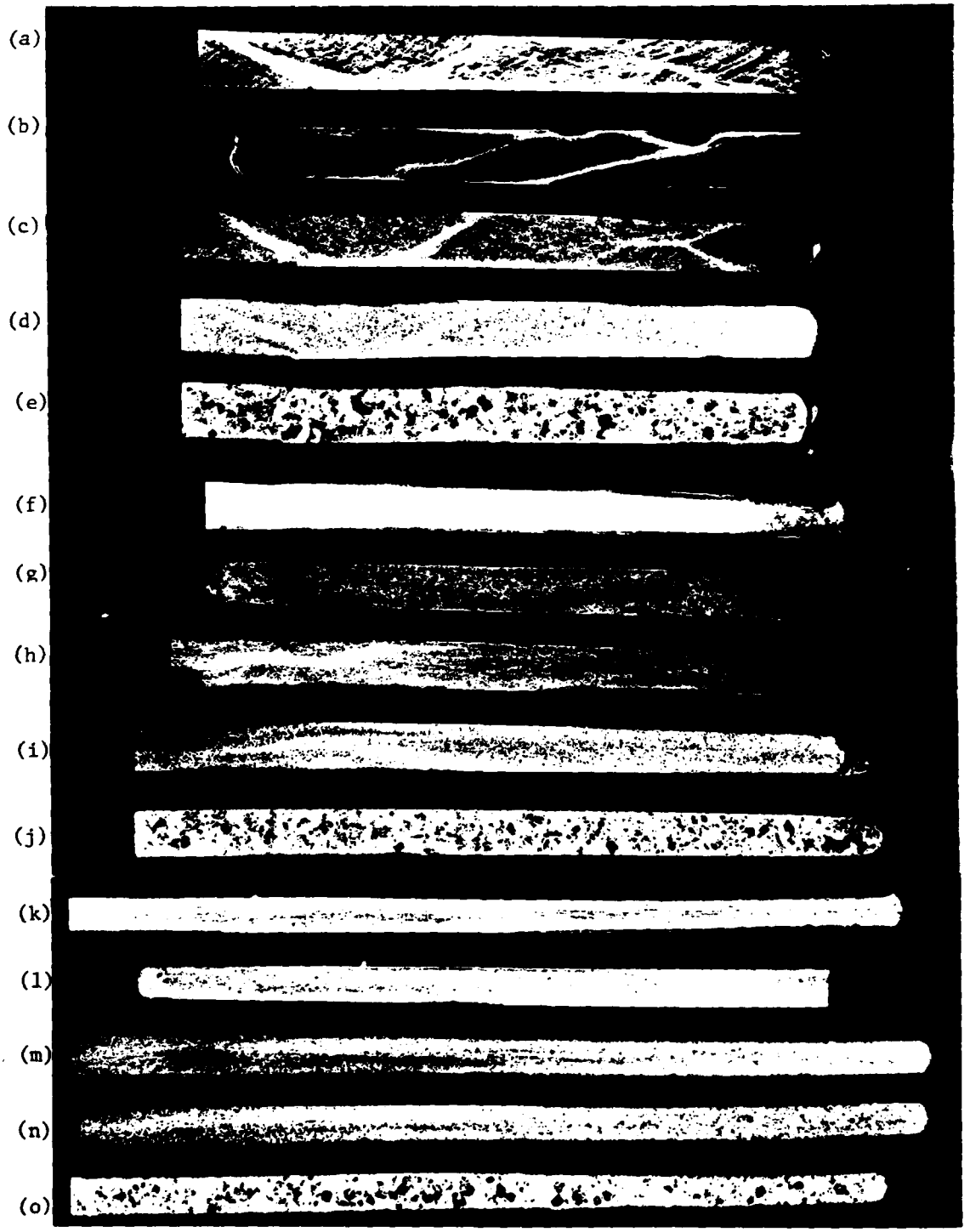

FIGURE 23. Transverse Metallographic Sections of α+β Preform Microstructure Flat Forgings. Preform Temperature/Die Temperature/Dwell Time were (a-e) 913 C/191 C/10 Secs., (f-j) 982 C/191 C/10 Secs., (k-o) 982 C/371 C/ 0 Secs. Macrostructures (a,f,k) are As-Forged. Other Forgings were Solution-Annealed for 1 Hour (Prior to Aging Treatment of 593 C/8 Hrs.) at (b,g,l) 899 C, (c,h,m) 954 C, (d,i,n) 979 C, (e,j,o) 1010 C. (3.5X)

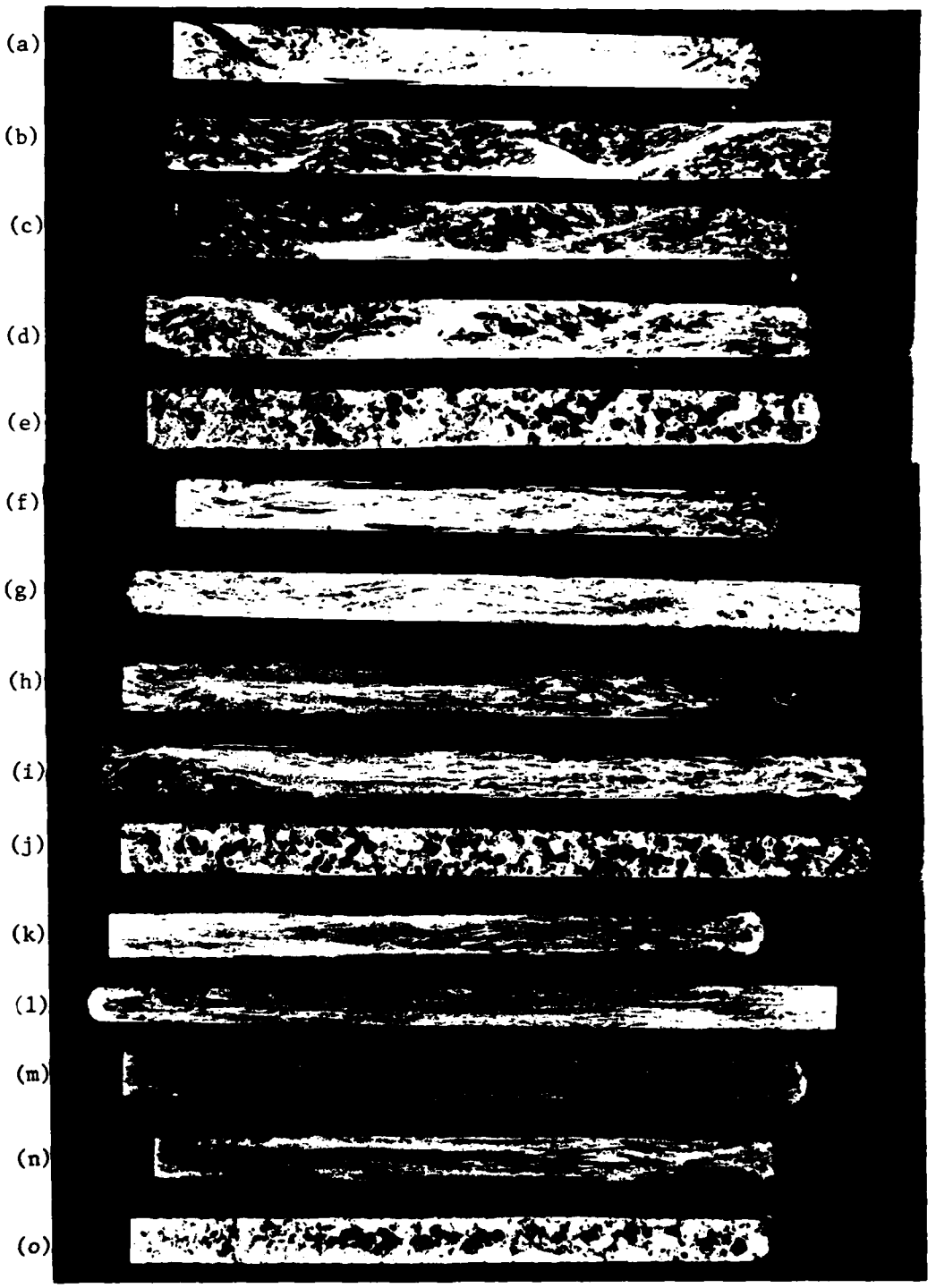

FIGURE 24. Transverse Metallographic Sections of β Preform Microstructure Flat Forgings. Preform Temperature/Die Temperature/Dwell Time were (a-e) 913 C/191 C/10 Secs., (f-j) 982 C/191 C/10 Secs., (k-o) 982 C/371 C/ 0 Secs. Macrostructures (a,f,k) are As-Forged. Other forgings were Solution-Annealed for 1 Hour (Prior to Aging Treatment of 593 C/8 Hrs.) at (b,g,l) 899 C, (c,h,m) 954 C, (d,i,n) 979 C, (e,j,o) 1010 C. (3.5X)

As a result of this work, two forging-heat treatment conditions which led to shear bands of different severity and two which led to microstructures with little, if any, shear localization were selected for each preform microstructure (Table 1). Additional flat forgings for mechanical property characterization were then made by sidepressing 1.52 cm (0.6 in.) diameter, 7.62 cm (3.0 in.) long preforms in the mechanical press using the various combinations of preform-preheat temperature, die temperature, and dwell time.

Evaluation of Tensile Properties

The effects of shear bands on tensile properties were evaluated to establish whether they may have deleterious effects on service performance. These and subsequent mechanical tests were performed at 510 C (950 F) since this is the design operating temperature of many Ti-6242 jet engine compressor parts, which are among the main applications of the alloy.

Duplicate flat tensile specimens, each with a 1.52 cm (0.6 in.) long, 0.64 cm (0.25 in.) wide gage section, were cut from each of two perpendicular directions in the forging for each forging-heat treatment condition. One of the directions was parallel to the preform bar axis (the nominal plane-strain direction in sidepressing) and is denoted as the "longitudinal" (L) direction in subsequent discussion. When loaded axially, these specimens would develop no shear stress on shear bands which may have been introduced during forging. The other test direction, denoted as "transverse" (T) in subsequent discussion, was perpendicular to the preform bar axis and is parallel to the long direction in the so-called transverse metallographic sections shown in Figures 23 and 24. Under axial loading along this direction, shear bands in the microstructure would have shear stress components imposed along them. During tensile specimen machining, approximately 0.25 mm (0.010 in.) was removed by milling and light mechanical polishing from each surface in order to eliminate alpha case as well as to make the surfaces flat and parallel. This was done, of course, for creep and fatigue specimens as well. After machining, tensile specimens were induction heated to test temperature and pulled in an MTS machine run at a constant crosshead speed of 0.51 cm/min. (0.2 in./min.). Some of the specimens were pulled to failure and others just short of it.

Tensile data (Table 2) demonstrated that the effect of shear bands on tensile properties is quite small. This is particularly evident when comparing L and T (longitudinal and transverse) data for a particular condition. First of all, it is seen that yield and ultimate strength data are comparable for L and T tests. This is as expected even for conditions with shear bands since defects, such as inclusions, usually have a noticeable effect only on fracture-related properties such as elongation and reduction in area. However, even the elongation data do not show a large effect that can be attributed to shear bands. The elongation values in samples with shear bands are comparable to ones reported previously for Ti-6242 alloy forgings[16]. Furthermore, the data for samples without shear bands suggest that differences in L and T data for samples with shear bands should be attributed to other sources such as data scatter or microscopic mechanical fibering.

Metallography supported the conclusions. In no cases could shear bands be associated in some systematic way with localized necking or fracture (Figures 25, 26, 27). It was found that in no samples were fracture paths found to lie along shear bands. One explanation for this may lie in hardness data taken on the mechanical property samples (Table 3). These hardness readings were taken inside and outside the gage section both in the bulk as well as within the shear bands themselves. Although there was a systematic variation of hardness between the shear bands and the bulk, the data taken in the gage section were almost identical to those outside the gage section, suggesting a minimal amount ot work-hardening. However, the data do show a definite trend that suggests the shear bands are harder than the surrounding bulk. This would explain perhaps why localized necks, and hence, the fractures resulting from the necks, occur in regions not associated with shear bands or in regions in which the resolved shear stress component is low along the shear band.

Evaluation of Creep Properties

The evaluation of the effects of shear bands on creep properties was performed with the objective of establishing service performance characteristics when this failure mode is operative. Flat creep specimens similar to the tensile specimens were prepared from forgings and tested in air under

TABLE 2. Tensile Data Obtained at 510 C

Preform Microstructure	Forging Parameters: Preheat Temp. (C)/ Die Temp. (C)/ Dwell Time (secs.)/	Solution Annealing Temp. (C)/ Shear Band Rating+	Tensile Test Direction	Yield Strength (MPa(KSI))	UTS (MPa(KSI))	Total Elongation (pct.)
α+β	913/191/10	899/1	L	621 (90.1)	785 (113.9)	11
α+β	913/191/10	899/1	T	584 (84.7)	741 (107.4)	17
α+β	913/191/10	954/2	L	611 (88.6)	785 (113.8)	7
α+β	913/191/10	954/2	T	645 (93.5)	860 (124.8)	6
α+β	982/191/10	954/3	L	692(100.3)	865 (125.4)	13
α+β	982/191/10	954/3	T	603 (87.5)	807 (117.1)	13
α+β	982/371/0	954/3	L	788(114.3)	904 (131.1)	7
α+β	982/371/0	954/3	T	682 (98.9)	867 (125.7)	16
β	913/191/10	899/1.75	L	718(104.2)	849 (123.2)	7
β	913/191/10	899/1.75	T	516 (74.8)	763 (110.7)	9
β	913/191/10	954/2	L	739(107.2)	945 (137.1)	6
β	913/191/10	954/2	T	706(102.4)	917 (133.0)	6
β	982/191/10	954/3	L	704(102.1)	857 (124.3)	11
β	982/191/10	954/3	T	730(105.9)	922 (133.7)	7
β	982/371/0	954/3	L	829(120.2)	1025 (148.6)	14
β	982/371/0	954/3	T	746(108.2)	898 (130.3)	8

+ See Table 1 for Qualitative Shear Band Rating System Explanation

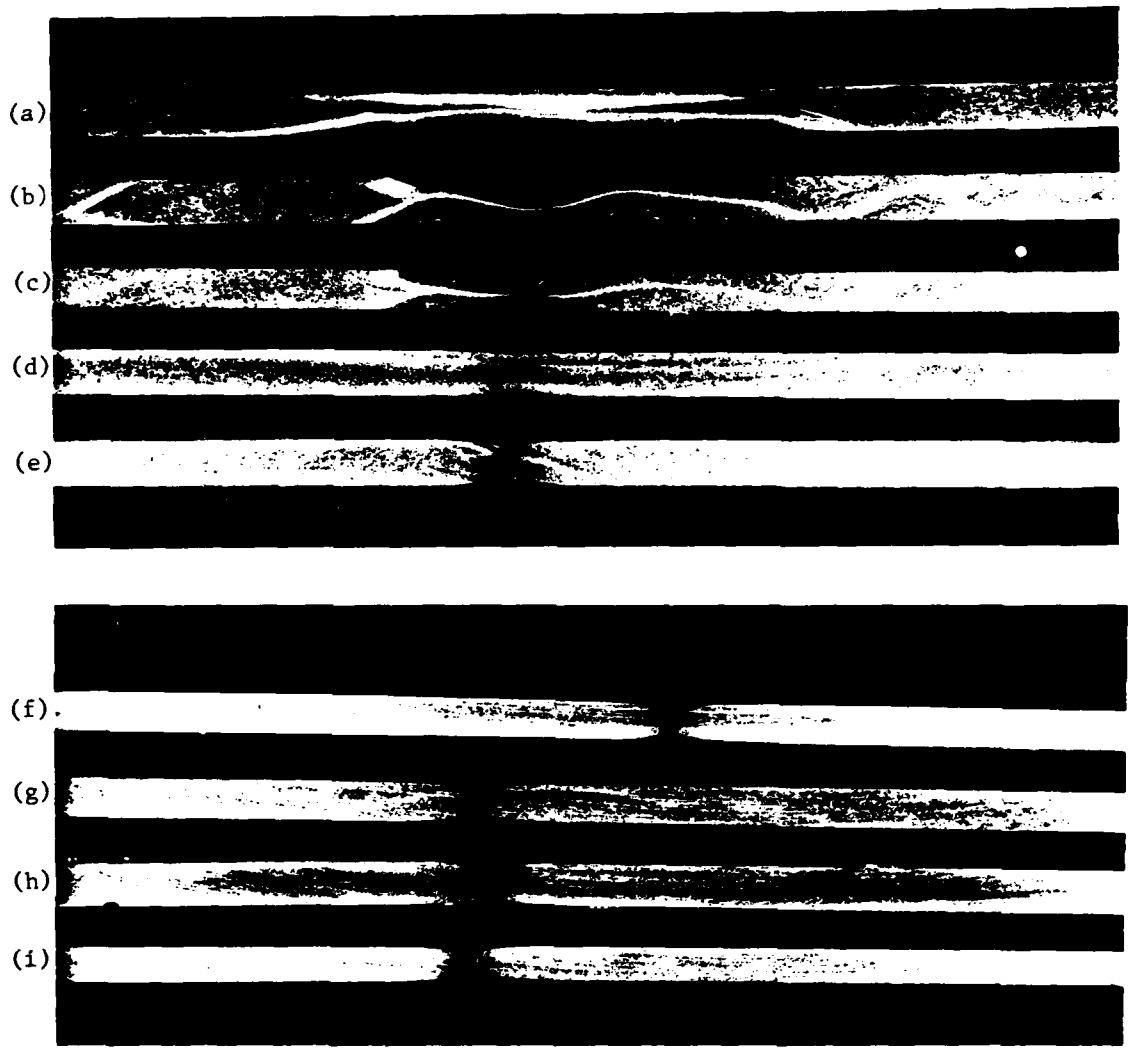

FIGURE 25. Tensile Axis Sections of α+β Preform Microstruction 510 C Tensile Samples Cut from Forgings. Forging Temperatures were (a-e) 913 C, (f-i) 982 C; Die Temperatures were (a-g) 191 C, (h,i) 371 C; Dwell Times were (a-g) 10 Secs., (h,i) 0 Secs. Solution Treatment (Prior to Aging Treatment of 593 C/8 Hrs.) was Performed for 1 Hour at (a-c) 899 C or (d-i) 954 C. Tensile Axis Directions were (a,d,f,h) Longitudinal or (b,c,e,g,i) Transverse. (3X)

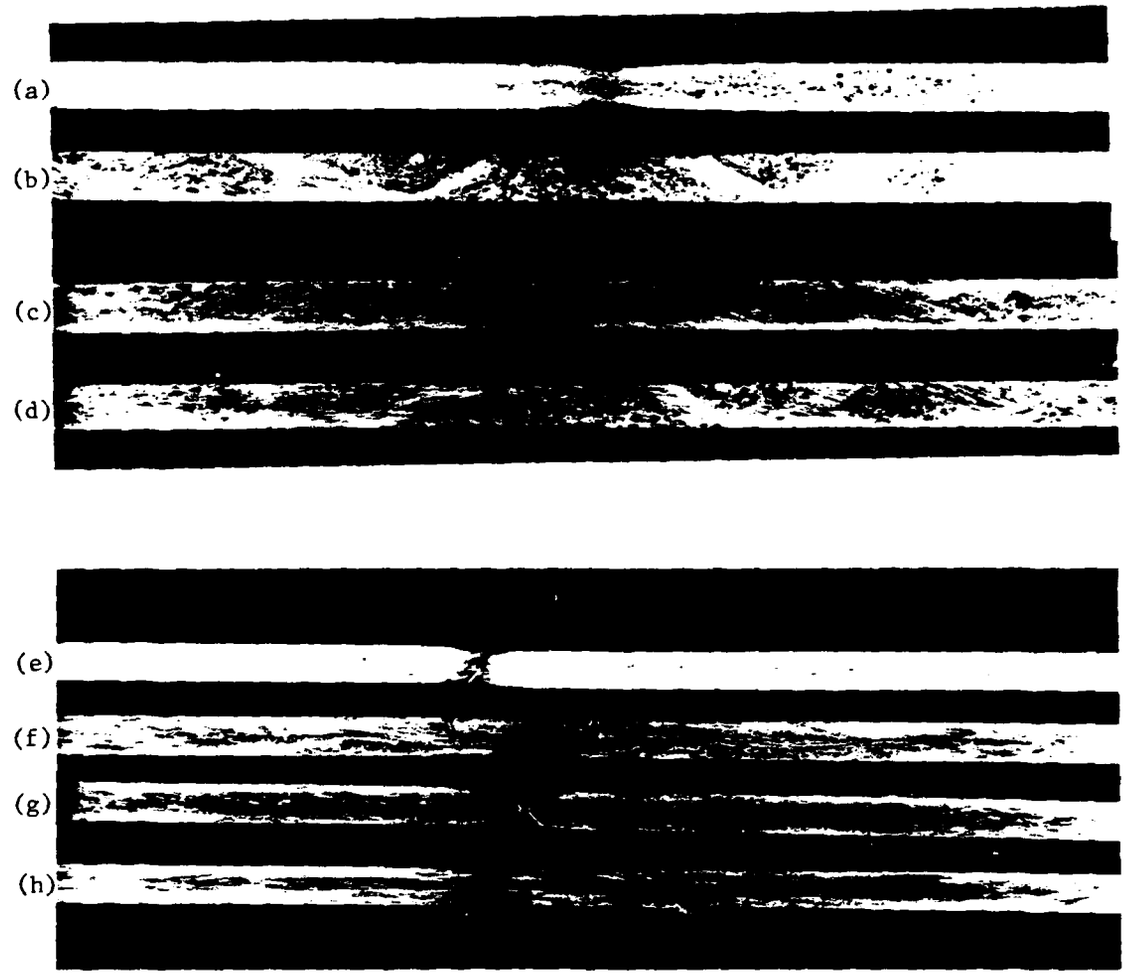

FIGURE 26. Tensile Axis Sections of β Preform Microstructure 510 C Tensile Samples Cut from Forgings. Forging Temperatures were (a-d) 913 C, (e-h) 982 C; Die Temperatures were (a-f) 191 C, (g,h) 371 C; Dwell Times were (a-f) 10 Secs., (g,h) 0 Secs. Solution Treatment (Prior to Aging Treatment of 593 C/8 Hrs.) was Performed for 1 Hour at (a,b) 899 C or (c-h) 954 C. Tensile Axis Directions were (a,c,e,g) Longitudinal or (b,d,f,h) Transverse. (3X)

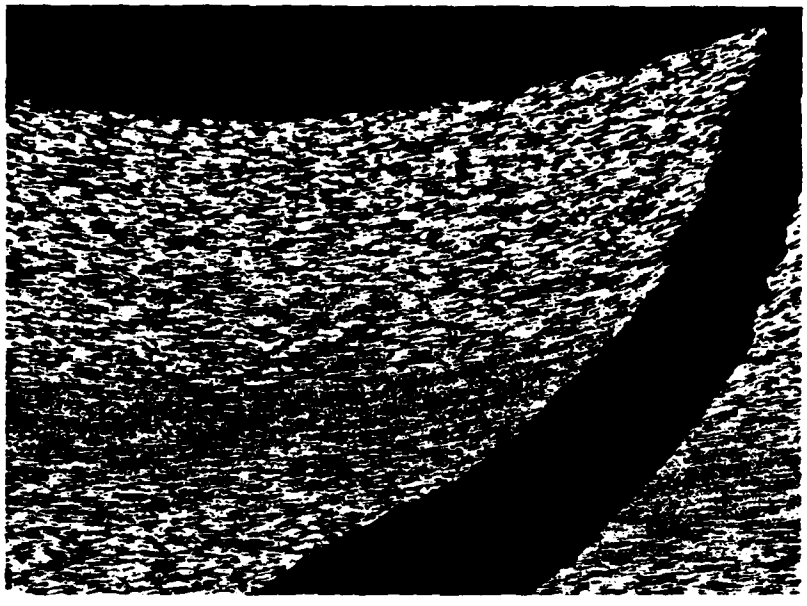

Tensile
Axis

FIGURE 27. Micrograph at Fracture of Transverse 510 C Tensile Sample Showing Fracture Path and Shear Band. Sample was Cut from $\alpha+\beta$ Microstructure Forging (Preheat Temperature 913 C, Die Temperature 191 C, Dwell Time 10 Secs.) which had been Solution Treated at 899 C for 1 Hour and Aged at 593 C for 8 Hours. (100X)

TABLE 3. Knoop Hardness Readings (500 Gram Load) Taken on Mechanical Property Specimens

Type of Specimen	Preform Microstructure	Forging Parameters: Preheat Temp. (C)/ Die Temp. (C)/ Dwell Time (secs.)	Solution Annealing Temp. (C)	Test Direction	UTS or Creep Stress or Max. Fatigue Stress (MPa(KSI))	Knoop Hardness Outside Shear Band	Knoop Hardness Inside Shear Band
Tensile	α+β	913/191/10	899	T	762(110.5)	367	399
Tensile	α+β	913/191/10	954	T	860(124.8)	393	403
Tensile	β	913/191/10	899	T	787(114.2)	371	377
Creep	α+β	913/191/10	899	T	552 (80)	381	405
Creep	β	913/191/10	899	T	517 (75)	389	405
Fatigue	α+β	913/191/10	899	T	448 (65)	349	384
Fatigue	β	913/191/10	899	T	483 (70)	363	386
Fatigue	α+β	982/371/0	954	L	414 (60)	408	-

constant load conditions (constant nominal stress) in a resistance furnace. Creep curves (Figures 28 and 29) and rupture life data (Table 4) were obtained at 510 C (950 F) using standard techniques.

Creep data on samples with shear bands demonstrated that creep performance can be definitely affected deleteriously. Inspection of the data shows that the effects of L vs. T loading are noticeable in creep rates and rupture lives, with T properties being poorer. The total magnitude of the effect, however, is not realized until the data for samples without shear bands are also examined. In these data, L properties are inferior to T properties, suggesting other mechanical texturing effects. Therefore, without these additional mechanical texturing effects, data for the samples with shear bands might have been expected to show even greater divergence in L vs. T properties.

The source of the effect of shear bands on creep properties was not evident from metallographic observations (Figures 30, 31, 32). As with the tensile data, in T samples with shear bands, the fracture path was not found to lie along the shear bands. The only other possible explanation for the observations thus must lie with some microscopic process such as enhanced diffusion along shear bands, diffusion which may be further increased by the action of imposed shear stresses (in T specimens) in creep. This would explain the increased creep rates as well as perhaps the shorter rupture lives of T samples containing shear bands. This hypothesis needs to be justified with further research though.

Evaluation of Fatigue Properties

The evaluation of the effects of shear bands on fatigue properties was performed with the objective of establishing service performance characteristics when this failure mode is operative. Flat fatigue specimens similar to the tensile and creep specimens were prepared from forgings and tested in air in load-control, tension-tension fatigue in an MTS machine at 510 C (950 F). Initially, strain-controlled fatigue tests were planned, but when it was found that the alloy shows negligible cyclic hardening or softening at 510 C (950 F),[17] it was decided to perform load-control tests because these would not require special devices to prevent buckling. The actual

(a)

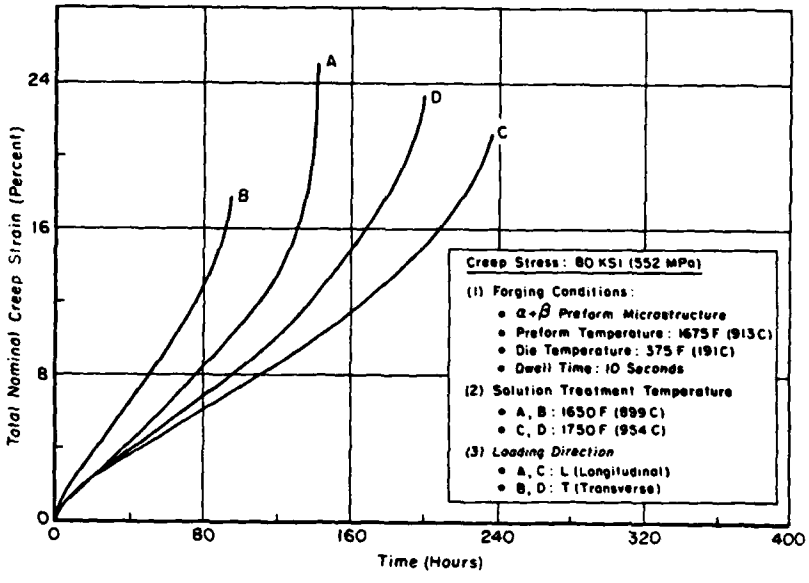

(b)

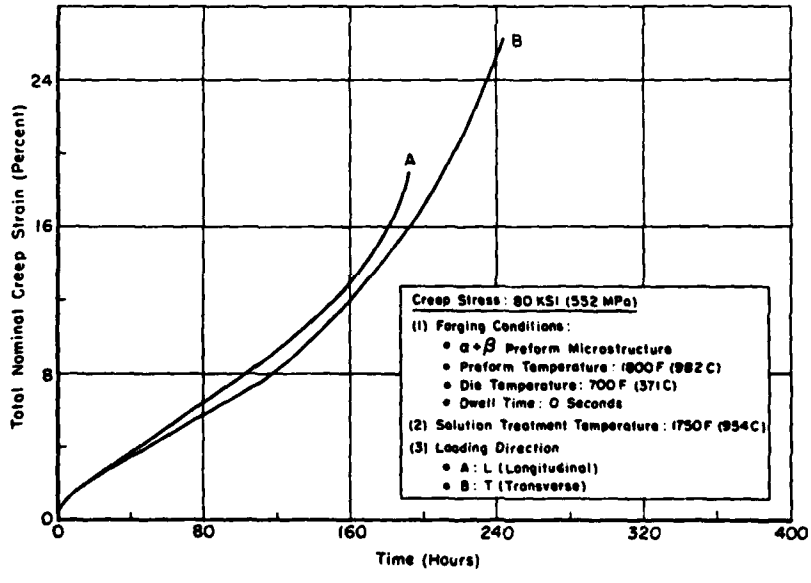

FIGURE 28. Constant-Load Creep Data for Samples Cut from α+β Preform Microstructure Forgings in which (a) There Were and (b) There Were Not Shear Bands.

(a)

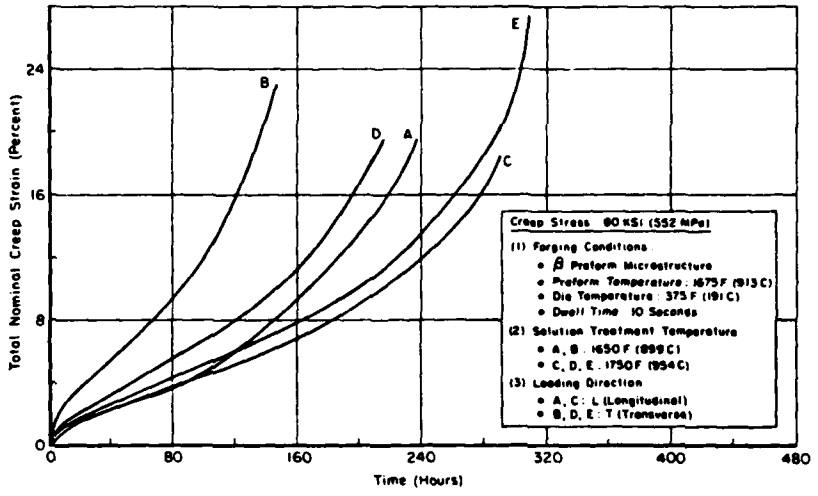

(b)

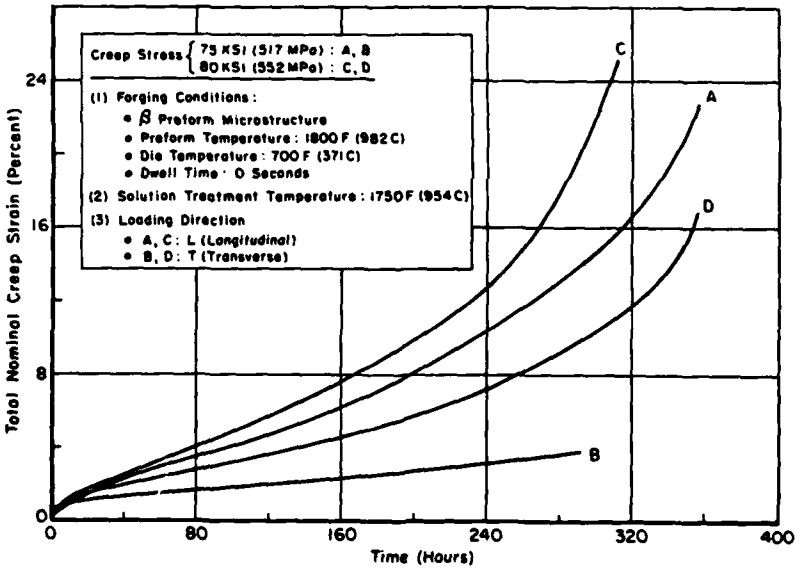

FIGURE 29. Constant-Load Creep Data for Samples Cut from β Preform Microstructure Forgings in which (a) There Were and (b) There Were Not Shear Bands.

TABLE 4. Creep Data Obtained at 510 C

Preform Microstructure	Forging Parameters: Preheat Temp. (C)/ Die Temp. (C)/ Dwell Time (secs.)	Solution Annealing Temp. (C)/ Shear Band Rating+	Creep Stress (MPa(KSI))	Creep Test Direction	Rupture Life (hrs.)	Nominal Creep Elongation (pct.)
α+β	913/191/10	899/1	379 (55)	L	1388	44
α+β	913/191/10	899/1	379 (55)	T	1382	46
α+β	913/191/10	899/1	552 (80)	L	146	38
α+β	913/191/10	899/1	552 (80)	T	117	42
α+β	913/191/10	954/2	552 (80)	L	261	40
α+β	913/191/10	954/2	552 (80)	T	226	34
α+β	982/371/0	954/3	552 (80)	L	208	32
α+β	982/371/0	954/3	552 (80)	T	245	28
β	913/191/10	899/1.75	517 (75)	L	310	45
β	913/191/10	899/1.75	517 (75)	T	281	34
β	913/191/10	899/1.75	552 (80)	L	259	38
β	913/191/10	899/1.75	552 (80)	T	149	28
β	913/191/10	954/2	552 (80)	L	299	33
β	913/191/10	954/2	552 (80)	T	260	27
β	982/371/0	954/3	517 (75)	L	372	25
β	982/371/0	954/3	517 (75)	T	483	24
β	982/371/0	954/3	552 (80)	L	318	36
β	982/371/0	954/3	552 (80)	T	321	23

+See Table 1 for Qualitative Shear Band Rating System Explanation

FIGURE 30. Creep Axis Sections of α+β Preform Microstructure 510 C Creep Samples Cut from Forgings. (Nominal Creep Stress: 552 MPa (80 KSI)). Forging Temperatures were (a-e) 913 C, (f,g) 982 C; Die Temperatures were (a-e) 191 C, (f,g) 371 C; Dwell Times were (a-e) 10 Secs., (f,g) 0 Secs. Solution Treatment (Prior to Aging Treatment of 593 C/8 Hrs.) was Performed for 1 Hour at (a,b) 899 C or (c-g) 954 C. Creep Axis Directions were (a,c,f) Longitudinal or (b,d,e,g) Transverse. (3X)

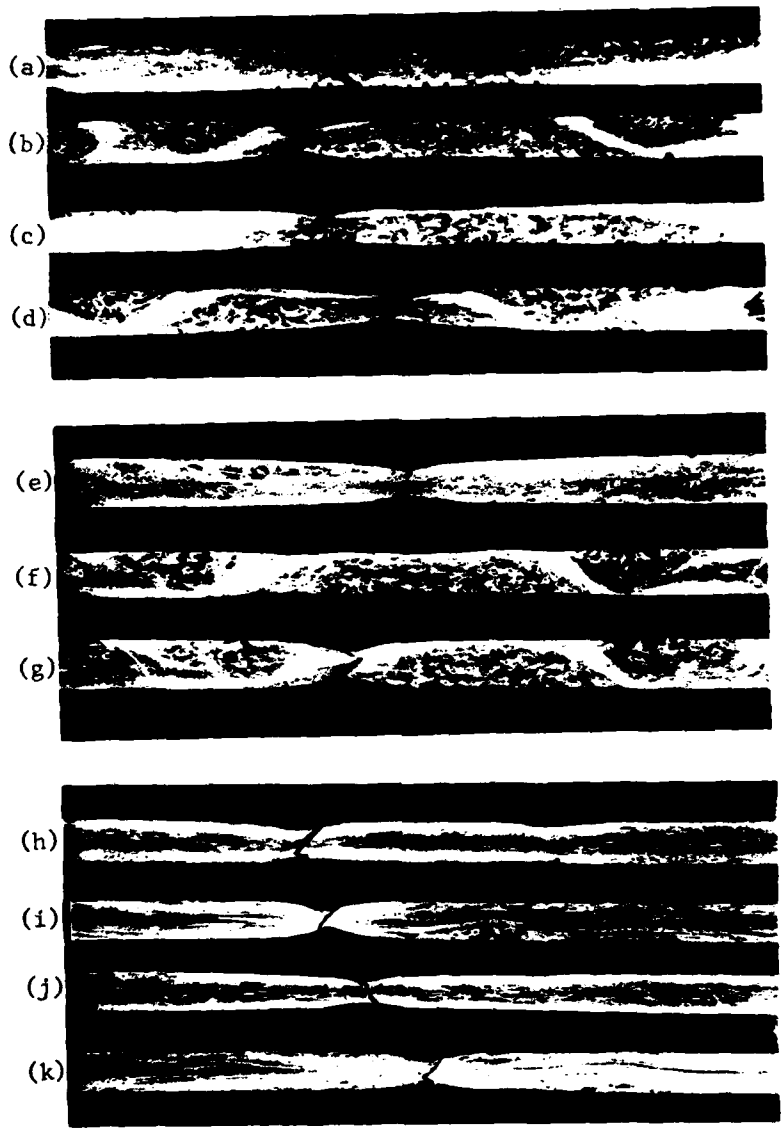

FIGURE 31. Creep Axis Sections of β Preform Microstructure 510 C Creep Samples Cut from Forgings (Nominal Creep Stress: (a,b,h,i) 517 MPa (75 KSI), (c-g,j,k) 552 MPa (80 KSI)). Forging Temperatures were (a-g) 913 C, (h-k) 982 C; Die Temperatures were (a-g) 191 C, (h-k) 371 C; Dwell Times were (a-g) 10 Secs., (h-k) 0 Secs. Solution Treatment (Prior to Aging Treatment of 593 C/8 Hrs.) was Performed for 1 Hour at (a-d) 899 C or (e-k) 954 C. Creep Axis Directions were (a,c,e,h,j) Longitudinal or (b,d,f,g,i,k) Transverse. (3X)

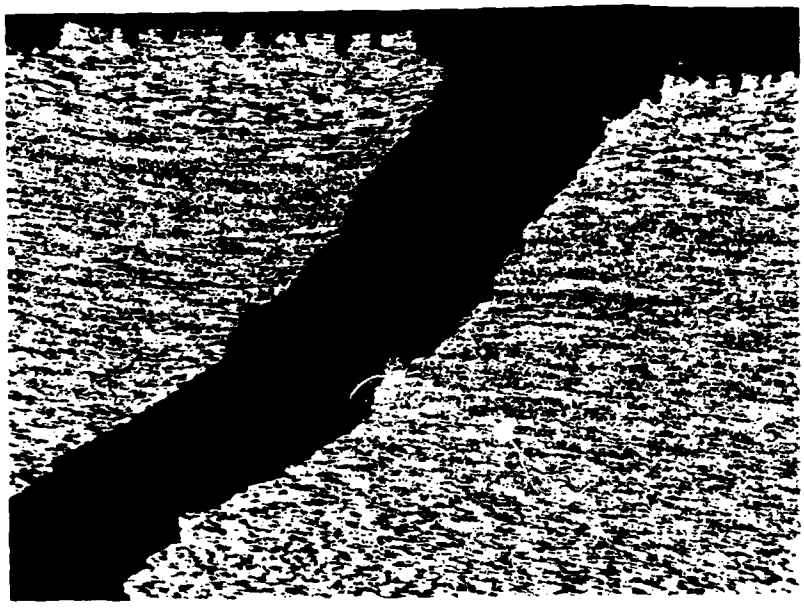

FIGURE 32. Micrograph at Fracture of Transverse 510 C Creep Sample (Creep Stress = 379 MPa (55 KSI)) Showing Fracture Path and Shear Band. Sample was Cut from $\alpha+\beta$ Microstructure Forging (Preheat Temperature 913 C, Die Temperature 191 C, Dwell Time 10 Secs.) which had been Solution Treated at 899 C for 1 Hour and Aged at 593 C for 8 Hours. (100X)

fatigue tests were run using induction heating with an R value (ratio of minimum to maximum stress) of +0.1 and and cyclic frequency of 5 Hz.

Fatigue data (Table 5) established no clear-cut effect of shear bands on fatigue lives. Although the L lives were usually longer than the T lives in samples with shear bands, the difference was small and must be considered to be due to the data scatter inherent in fatigue testing. Also in support of this conclusion, is the fact that samples without shear bands showed data scatter as well and no pattern of L properties being either better or worse than T properties. Furthermore, metallography demonstrated that neither fracture initiation sites nor fracture paths could be associated with shear bands (Figures 33 and 34).

One plausible explanation of the lack of an effect of shear bands may be that the shear bands are harder than the bulk (Table 3) and that it is thus easier to initiate and propagate a crack in the bulk. If this were the case, L and T properties in samples with shear bands would be both representative of bulk properties, especially since the tests were run in load control. It is conceivable that the results would be different if fatigue testing were done in strain control since T samples with shear bands might have shorter effective gage lengths because of the hardness effect.

TABLE 5. Fatigue Data Obtained at 510 C

Preform Microstructure	Forging Parameters: Preheat Temp. (C)/ Die Temp. (C)/ Dwell Time (secs.)	Solution Annealing Temp. (C)/ Shear Band Rating+	Max. Fatigue Stress (MPa(KSI))	Fatigue Test Direction	Cycles to Failure
α+β	913/191/10	899/1	414 (60)	L	19,620
α+β	913/191/10	899/1	414 (60)	T	14,820
α+β	913/191/10	899/1	483 (70)	L	13,150
α+β	913/191/10	899/1	483 (70)	T	10,475
α+β	913/191/10	954/2	483 (70)	L	10,435
α+β	913/191/10	954/2	483 (70)	T	8,145
α+β	982/371/0	954/3	414 (60)	L	21,355
α+β	982/371/0	954/3	414 (60)	T	9,385
α+β	982/371/0	954/3	483 (70)	L	9,260
α+β	982/371/0	954/3	483 (70)	T	26,310
β	913/191/10	899/1.75	483 (70)	L	12,985
β	913/191/10	899/1.75	483 (70)	T	10,240
β	913/191/10	954/2	483 (70)	L	7,025
β	913/191/10	954/2	483 (70)	T	16,420
β	982/371/0	954/3	483 (70)	L	8,300
β	982/371/0	954/3	483 (70)	T	25,865

+ See Table 1 for Qualitative Shear Band Rating System Explanation

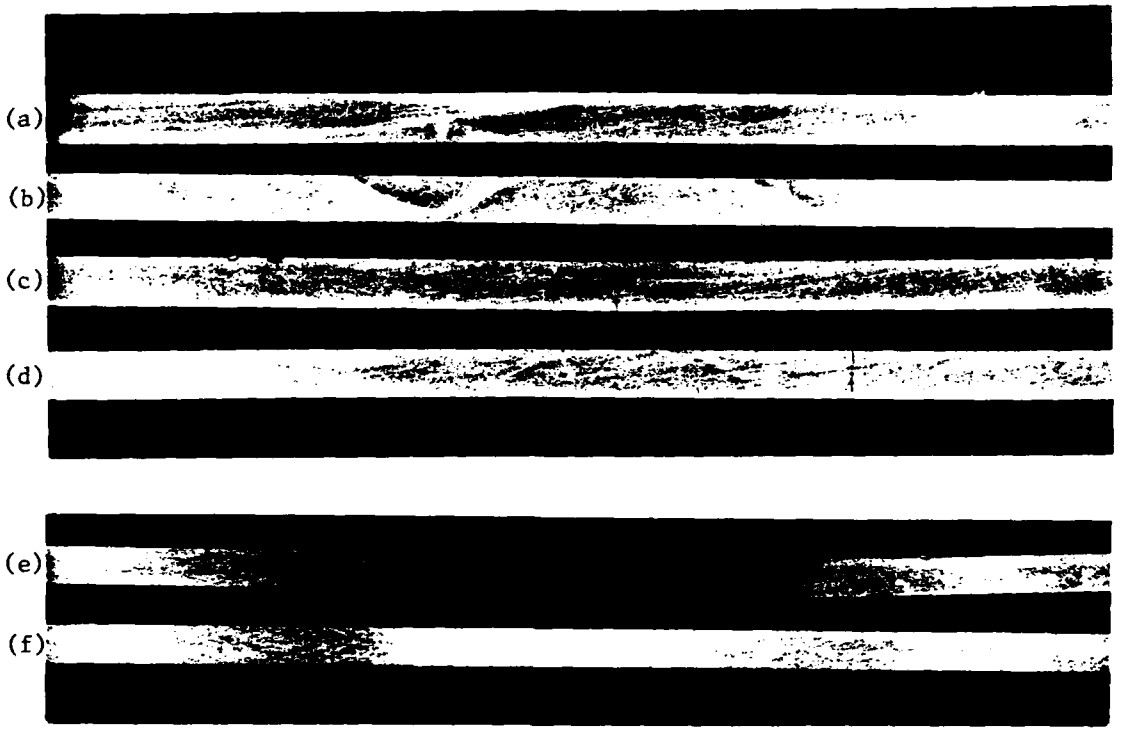

FIGURE 33. Fatigue Axis Sections of α+β Preform Microstructure 510 C Fatigue Samples Cut from Forgings (Fatigue Stress: 483 MPa (70 KSI)). Forging Temperatures were (a-d) 913 C, (e,f) 982 C; Die Temperatures were (a-d) 191 C, (e,f) 371 C; Dwell Times were (a-d) 10 Secs., (e,f) 0 Secs. Solution Treatment (Prior to Aging Treatment of 593 C/8 Hrs.) was Performed for 1 Hour at (a,b) 899 C or (c-f) 954 C. Fatigue Axis Directions were (a,c,e) Longitudinal or (b,d,f) Transverse. (3X)

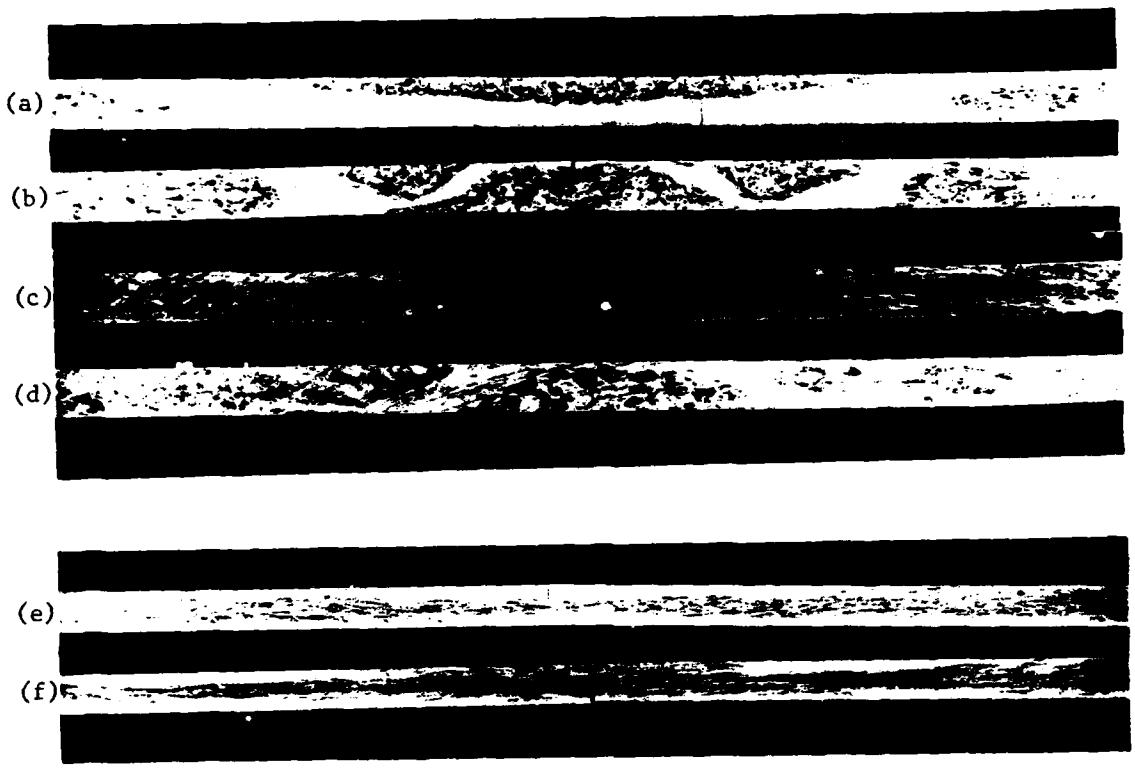

FIGURE 34. Fatigue Axis Sections of β Preform Microstructure 510 C Fatigue Samples Cut from Forgings (Fatigue Stress: 483 MPa (70 KSI)). Forging Temperatures were (a-d) 913 C, (e,f) 982 C; Die Temperatures were (a-d) 191 C, (e,f) 371 C; Dwell Times were (a-d) 10 Secs., (e,f) 0 Secs. Solution Treatment (Prior to Aging Treatment of 593 C/8 Hrs.) was performed for 1 Hour at (a,b) 899 C or (c-f) 954 C. Fatigue Axis Directions were (a,c,e) Longitudinal or (b,d,f) Transverse. (3X)

CONCLUSIONS

The results of this program provide a unique understanding of required practices and precision attainable without the occurrence of shear band defects for isothermal forging (typically done in "show" hydraulic presses) and conventional forging (done in mechanical and hydraulic presses). In isothermal forging, low working speed is beneficial from the viewpoints of lower working loads, the generally higher strain-rate sensitivity of materials hot worked at low strain rates, and the minimization of deformation-induced heating and thermal softening. It has been demonstrated that large rate sensitivities and small levels of flow softening both counteract the tendency to form shear bands under nominally isothermal conditions. In non-isothermal forging, it has been shown that heat transfer can have a significant effect on forgeability. This is important since large amounts of heat transfer can lead to working at temperatures at which the material has inherently low workability. In addition, large temperature gradients across the workpiece may be developed. These gradients may lead to large deformation gradients and hence, shear bands in materials with flow stresses which are heavily termperature dependent, such as titanium alloys. It is significant to note that near-net shape or precision forging of titanium alloy parts is normally only done conventionally in mechanical presses or isothermally in hydraulic presses. Further development of the presented simulation capabilities for use on other forging geometries could provide a quantitative basis for determining the necessary conditions (including required die temperatures) for forging shapes in mechanical and hydraulic presses in order to minimize loads and avoid defects. This technical input would be critical for producing acceptable quality forgings at the lowest possible cost.

This program has also established the effect of shear bands on service properties for Ti-6242 forgings. Although the effect is small or negligible for tensile and fatigue loadings, creep properties may be noticeably degraded by shear bands. Mechanisms by which this degradation occurs have been suggested, but further research is needed to verify them.

PRESENTATIONS AND PUBLICATIONS

- S. L. Semiatin and G. D. Lahoti, "Unstable Flow in Hot Forging of Titanium Alloys", presentation at Fall Meeting, TMS-AIME, Milwaukee, Wisconsin (September, 1979).
- S. L. Semiatin and G. D. Lahoti, "Shear Band Development in Hot Working of Titanium Alloys", presentation at AIME Annual Meeting, Chicago, Illinois (February, 1981).
- G. D. Lahoti and S. L. Semiatin, "Application of Process Modeling to Predict Microstructural Response in Hot Forging of a Two-Phase Titanium Alloy", paper presented at and published in proceedings of Ninth AIMTDR Conference, December, 1980.
- S. L. Semiatin and G. D. Lahoti, "Deformation and Unstable Flow in Hot Torsion of Ti-6Al-2Sn-4Zr-2Mo-0.1Si", Met. Trans. A, 1981, Vol. 12A, p 1719.
- S. L. Semiatin and G. D. Lahoti, "Deformation and Unstable Flow in Hot Forging of Ti-6Al-2Sn-4Zr-2Mo-0.1Si", Met. Trans. A, 1981, Vol. 12A, p 1705.
- S. L. Semiatin and G. D. Lahoti, "Forging of Metals", Scientific American, 1981, Vol. 245, No. 2, p 98.
- S. L. Semiatin and G. D. Lahoti, "The Occurrence of Shear Bands in Isothermal, Hot Forging", Met. Trans. A, 1982, Vol. 13A, p 275.
- S. L. Semiatin and G. D. Lahoti, "The Occurrence of Shear Bands in Non-Isothermal, Hot Forging", paper in preparation for submission to Met. Trans.
- S. L. Semiatin and G. D. Lahoti, "The Effect of Shear Bands on Service Properties of Ti-6242 Forgings", paper in preparation for submission to Met. Trans.
- C. R. Thompson and S. L. Semiatin, "The Occurrence of Shear Bands in Isothermal, Hot Forging", exhibit prepared for 1980 International Metallographic Exhibit (sponsored by IMS and ASM).

LIST OF PERSONNEL

(1) Dr. S. L. Semiatin, Metalworking Section

(2) Dr. G. D. Lahoti, Metalworking Section

(3) Dr. S. I. Oh, Metalworking Section

(4) Dr. A. L. Hoffmanner, Metalworking Section

(5) Dr. T. Altan, Engineering & Manufacturing Technology Department

COUPLING

Personnel at AFWAL (A. M. Adair and H. Gegel) have been kept aware of progress on the present project. They have been receiving preprints of the papers resulting from the program. In addition, the results have been presented at the Processing Science Program Workshops (July, 1980, August, 1981), at which various AFWAL, University, and industrial people were in attendance. Several presentations on project results have also been given at AFWAL. These project reviews met with favorable reaction from AFWAL personnel.

The engineers who worked on this project (S. L. Semiatin and G. D. Lahoti) have also worked closely together on the Dual Property Disk Program, and the results of the two projects have been coupled to enhance the significance of each program.

REFERENCES

1. G. D. Lahoti and T. Altan, Report AFML-TR-79-4156, Battelle-Columbus Laboratories, Columbus, Oh., 1979.

2. J. J. Jonas and M. J. Luton, Advances in Deformation Processing, J. J. Burke and V. Weiss, Editors, Plenum Press, N.Y., 1978. p 215.

3. D. J. Abson and J. J. Jonas, Met Techn., 1977, Vol. 4, p 462.

4. W. A. Backofen, Deformation Processing, Addison-Wesley Publishing Co., Reading, Ma., 1972, Chap. 10.

REFERENCES (Continued)

5. S. L. Semiatin and G. D. Lahoti, Met. Trans. A, 1981, Vol. 12A, p 1719.

6. S. L. Semiatin and G. D. Lahoti, Met. Trans A, 1982, Vol. 13A, p 275.

7. S. Kobayashi, C. H. Lee, and S. C. Jain, Report AFML-TR-70-90, University of California, Berkeley, Ca., 1970.

8. J. J. Jonas, R. A. Holt, and C. E. Coleman, Acta Met., 1976, Vol. 24, p 911.

9. S. I. Oh, Inter. J. Mech. Sci., 1982, Vol. 24 (in press).

10. M. N. Janardhana and S. K. Biswas, Inter J. Mech. Sci., 1979, Vol 21, p 699.

11. S. L. Semiatin, Unpublished Research For USAF (Contract F33615-78-C-5025) and Aerojet Ordnance Corp., Battelle-Columbus Laboratories, Columbus, Oh., 1979.

12. G. D. Lahoti and T. Altan, J. Eng. Materials and Techn., Trans. ASME, 1975, Vol. 97, p 113.

13. C. C. Chen, Report RD-77-110, Wyman Gordon Co., North Grafton, Ma., 1977.

14. J. Pepe, Technical Report WVT-7217, Watervliet Arsenal, Watervliet, N.Y., 1972.

15. J. Pepe, Met Trans., 1973, Vol. 4, p 2455.

16. G. D. Lahoti and T. Altan, Report AFML-TR-80-4162, Battelle-Columbus Laboratories, Columbus, Ohio, 1980.

17. J. E. Allison, J. C. Williams, S. L. Semiatin, Unpublished Research for USAF (Contract F33615-78-C-5025), Carnegie-Mellon University, Pittsburgh, Pa., and Battelle-Columbus Laboratories, Columbus, Ohio, 1981.

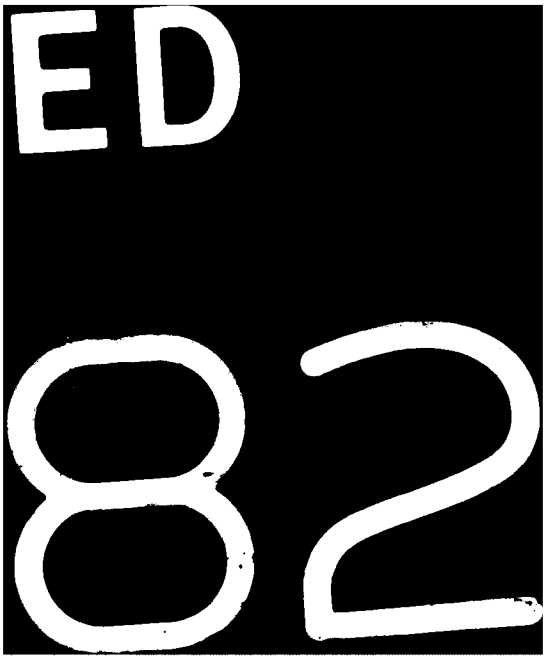
ED
82